Phase equilibrium in the system CaCO3–MgCO3–FeCO3

Article *in* Journal of Petrology · April 1987

DOI: 10.1093/petrology/28.2.389 · Source: OAI

2 authors, including:

Lawrence M Anovitz
Oak Ridge National Laboratory
187 PUBLICATIONS **3,622** CITATIONS

SEE PROFILE

Phase Equilibria in the System $CaCO_3$–$MgCO_3$–$FeCO_3$*

by L. M. ANOVITZ AND E. J. ESSENE

Department of Geological Sciences, The University of Michigan, Ann Arbor, Michigan 48109

(*Received 11 July 1985; revised typescript accepted 14 November 1986*)

Experimental data on phase relations in the $CaCO_3$–$MgCO_3$–$FeCO_3$ ternary by Goldsmith *et al.* (1962) are inconsistent with those of Rosenberg (1967). These inconsistencies cannot be reconciled by the pressure or temperature differences between the two sets of experiments. Available reversed experiments on the binary systems have been re-evaluated to yield consistent binary solvi. These data have been combined with analyses of natural carbonates to yield approximate ternary phase diagrams at 250, 400, 550, and 700 °C, and used to model ternary activity/composition relations for calcite- and dolomite-structure carbonates. An empirical model for thermometry with calcite-ferroan dolomite was derived from the ternary solvus by fitting an empirical equation to the calcite limb of the ternary solvus. This model appears to extend reliably to higher iron contents than the models of Bickle & Powell (1977) and Powell *et al.* (1984).

INTRODUCTION

Current interpretations of carbonate phase equilibria in the system $CaCO_3$-$MgCO_3$-$FeCO_3$ are based on several sets of experimental data (Harker & Tuttle, 1955; Graf & Goldsmith, 1958; Rosenberg, 1960, 1963*a*, *b*, 1967; Goldsmith & Heard, 1961; Goldsmith *et al.*, 1962, Goldsmith & Newton, 1969; *cf.* Goldsmith, 1983). Investigators have interpreted the metamorphic conditions of their field areas in terms of these experiments (e.g., Pinsent & Smith, 1975; Talantsev & Sazanov, 1979). Careful examination of the experimental data, however, suggests that inconsistencies exist which limit their usefulness. We have therefore undertaken to derive the phase relations for this system using natural assemblages and reversed experimental data. Examination of carefully selected compositional data for natural carbonates combined with experimental data allows construction of a self-consistent set of phase relations.

REVIEW OF EXPERIMENTAL RESULTS

The results of Goldsmith *et al.* (1962) at 600 °C and 15 kb and Rosenberg (1967) at 500 °C and 3 kb represent the closest experimental conditions attained between the two sets of experiments on the ternary system (Fig. 1). The three-phase field for coexisting calcite–siderite–ankerite inferred by Goldsmith *et al.* (1962) is significantly wider than that suggested by Rosenberg. Goldsmith *et al.* placed the ankerite corner of the triangle at $X_{Dol}^{FeCO_3} = 0{\cdot}208$, $X_{Dol}^{CaCO_3} = 0{\cdot}515$, $X_{Dol}^{MgCO_3} = 0{\cdot}277$ and Rosenberg (1967) placed it at $X_{Dol}^{MgCO_3} = 0{\cdot}115$, $X_{Dol}^{CaCO_3} = 0{\cdot}545$, $X_{Dol}^{FeCO_3} = 0{\cdot}340$. While the general form of the two phase diagrams is similar, any discrepancies should be carefully evaluated before using $CaCO_3$-$MgCO_3$-$FeCO_3$ phase equilibria to interpret metamorphic carbonates.

It is possible that the differences between the experiments of Goldsmith *et al.* (1962) and Rosenberg (1967) are due to differences in pressure or temperature. This was assumed by

* Contribution No. 423 from the Mineralogical Laboratory, Department of Geological Sciences, The University of Michigan.

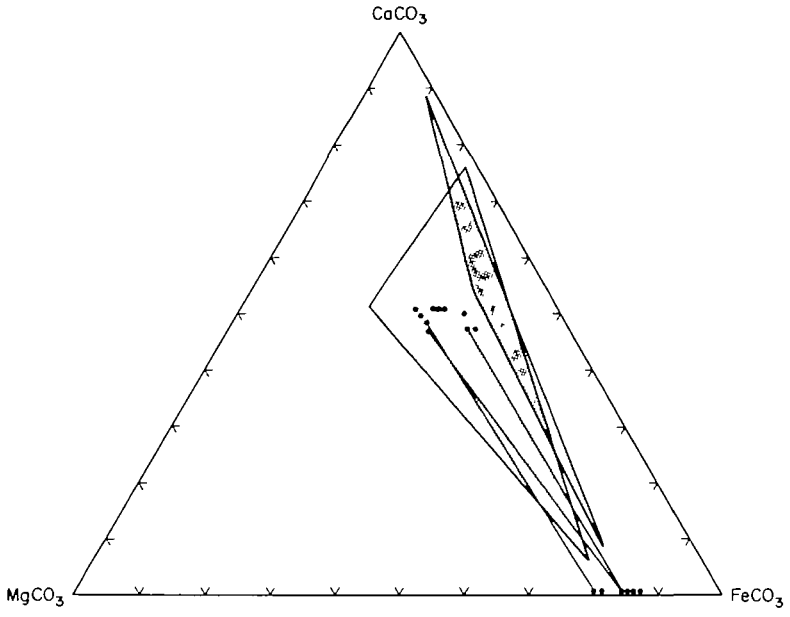

FIG. 1. The three-phase (calcite–ankerite–siderite) fields of by Rosenberg (1967) (narrow field) at 500 °C and 2 to 3 kb and Goldsmith *et al.* (1962) (wider field) at 600 °C and 15 kb, with selected natural ankerite and siderite analyses (Haase, 1979; Klein & Gole, 1981; our data, Wawa, Ontario). Data are in mol per cent, and tie-lines connect coexisting phases.

Talantsev & Sazonov (1979) who derived a pressure dependence for a carbonate thermometer by assuming both sets of experimental data to be correct. This may be thermodynamically tested by calculating which side of the reaction:

$$\text{Ankerite}_{ss}(1) = \text{Ankerite}_{ss}(2) + \text{Calcite}_{ss} + \text{Siderite}_{ss} \quad (1)$$

is stabilized by increased pressure or temperature. If we choose the composition of $\text{Ankerite}_{ss}(1)$ as the ankerite corner of the three-phase field defined by Rosenberg (1967), we may calculate its stability relative to Calcite_{ss}, Siderite_{ss} and a slightly more magnesian ankerite chosen for convenience [$\text{Ankerite}_{ss}(2)$, Table 1] using the tie-lines defined by Rosenberg (1967). Molar volumes for the ankerite solutions (Table 1) may be derived from the equations given by Goldsmith *et al.* (1962) and those for the calcite and siderite solutions by linear extrapolation into the ternary from data along the calcite–siderite and calcite–magnesite joins (Goldsmith *et al.*, 1962; Rosenberg, 1963; Robie *et al.*, 1978; Bischoff *et al.*, 1983). These approximations are necessary, as no data exist on the partial molar volumes of calcite-structure carbonates in the ternary system. Available binary data, however, show very small deviations from ideality, which suggests that errors in this approximation will not change the outcome of our calculations.

Using the carbonate compositions in Table 1, reaction (1) is balanced as:

$$\text{Ankerite}_{ss}(1) = 0{\cdot}903\ \text{Ankerite}_{ss}(2) + 0{\cdot}111\ \text{Calcite}_{ss} + 0{\cdot}083\ \text{Siderite}_{ss}, \quad (2)$$

for which $\Delta V_{298} = 0{\cdot}08\ \text{cm}^3\ \text{mol}^{-1}$. This volume change is small because of the similarity in composition of the two ankerites, but its positive sign means that ankerite will react with calcite and siderite to form a more iron-rich ankerite with increased pressure. As this result is opposite to that suggested by combination of Goldsmith's and Rosenberg's experiments, pressure differences cannot account for the differences in the observed results.

TABLE 1

Compositions and thermodynamic data for carbonate compositions used to calculate the effects of pressure and temperature on the position of the three-phase field

Phase	Composition X^{CaCO_3}	X^{MgCO_3}	X^{FeCO_3}	V°_{298} (cm^3 mol^{-1})	S°_{298} (J mol^{-1} K)
$Calcite_{ss}$	0·885	0·015	0·100	35·97	95·8
$Siderite_{ss}$	0·090	0·140	0·770	29·82	104·2
$Ankerite_{ss}$(1)	0·545	0·115	0·340	65·80	174·9
$Ankerite_{ss}$(2)	0·545	0·120	0·335	65·78	175·3
$CaFe(CO_3)_2$	0·500	0·000	0·500	65·72	168·2

In order to consider the effects of temperature on the three-phase field, the entropies for the phases must be known. End-member ankerite [$(CaFeCO_3)_2$] has never been found nor synthesized. Its entropy has been estimated (Fyfe & Verhoogen, 1958) as:

$$S^\circ_{298,\,Ank} = S^\circ_{298,\,Dol} - S^\circ_{298,\,Ms} + S^\circ_{298,\,Sd} + 2{\cdot}5\,\Delta V \text{ J mol}^{-1}\text{ K}^{-1}. \quad (3)$$

Data are taken from Robie *et al.* (1978, 1984). No data exist on the partial molar entropies of ternary carbonates, and the entropies of the solid-solutions were estimated using an ideal mixing model (Table 1). At constant pressure, using the reaction at equilibrium as the standard state:

$$RT\ln K \sim \Delta S \Delta T. \quad (4)$$

An ideal-ionic model was used to calculate the activities of the carbonate species; any deficiencies of this model are partly overcome by a tendency for the activity coefficients to cancel. For reaction (2), $K_D = 0{\cdot}988$ and $\Delta S = 2{\cdot}1$ J mol^{-1} K. Equation (4) may therefore be written:

$$R\ln K = -0{\cdot}10 \text{ J mol}^{-1}\text{ K}^{-1} \sim \Delta S \Delta T/T = 2{\cdot}1\Delta T/T \text{ (J mol}^{-1}\text{)},\ \Delta T = -0{\cdot}05T. \quad (5)$$

Again, the smallness of $R\ln K$ is due to the similarity in compositions between the two ankerites, but the ΔT *is* negative. Therefore, ankerite in equilibrium with calcite and siderite should become more ferroan with increased temperature and pressure, and the P/T differences between the Goldsmith and Rosenberg experiments do not explain the differences in their data.

Powell *et al.* (1984) attempted to experimentally redetermine the positions of tie-lines in the calcite–dolomite–ankerite solvus. Such a study should have provided an important check on the results of Goldsmith *et al.* (1962) and Rosenberg (1967). Unfortunately, the run products of Powell *et al.* contained fine grained intergrowths of calcite and ankerite yielding badly scattered microprobe analyses. While the authors tried to recover equilibrium data by statistical treatment of the results, such a procedure cannot distinguish disequilibrium information such as zoning or unambiguously identify the equilibrium assemblage. In addition, they used metastable mixtures of $CaCO_3$, $MgCO_3$ and $FeCO_3$ as starting materials. Goldsmith & Graf (1958) noted that it is difficult to use dolomite as a starting material due to its refractory nature. For this reason, magnesite rather than dolomite was used to supply the necessary magnesium for dolomite synthesis during their experiments. However, Byrnes & Wyllie (1981) note that mixtures of dry $CaCO_3$ and $MgCO_3$ are unsuitable starting materials for solvus measurements, despite their rapid reaction rates. Use

of calcite and magnesite to limit the position of the calcite–dolomite solvus requires that the rate of formation of ordered dolomite is faster than attainment of compositional equilibrium. If not, the experimental results may represent a metastable calcite–'disordered dolomite' or calcite–magnesite solvus. In experiments which begin with calcite, magnesite and siderite the final results may reflect the metastable calcite–magnesite–siderite solvus. In any case, experiments beginning with pure end-member phases are at best half-reversals which may not have attained equilibrium. We have therefore disregarded the results of Powell *et al.* (1984) in our evaluations.

The potential effects of the formation of metastable, partially ordered dolomite during experiments have been studied by Schultz-Güttler (1986). His experiments showed that the position of the solvus is strongly dependent on the ordering state of the dolomite, and that runs of up to 4 days were not long enough for the dolomite to reach its equilibrium ordering state even at 1000 °C. Unfortunately, Schultz-Güttler did not reverse the compositions of the calcite in equilibrium with each metastably disordered dolomite, and his suggested positions for the calcite limb of the solvus may be incorrect. In addition, periclase was present in most of the run products, requiring that the dolomite was breaking down to periclase, calcite, and CO_2. This neoformed calcite may not have attained the same composition as the calcite in the matrix. As calcite compositions were inferred from X-ray techniques, it is possible that the results represent an average of two populations of calcite compositions. This possibility should be checked by careful electron microprobe analyses of the run products.

Well-ordered starting materials were inferred by Schulz-Güttler (1986) to have partially disordered at 900 to 1000 °C on the basis of a decrease in the intensity of the 015 reflections. This change is difficult to reconcile with other work on ordering in dolomite (Reeder & Nakajima, 1982; Reeder, 1983) which suggested that at equilibrium dolomite is completely ordered at these temperatures. It is possible that much of the disordering inferred by Schultz-Güttler (1986) from his X-ray results is actually due to compositional changes in the dolomite. Analysis of his published *d*-values for 006 and 110 reflections suggests a decrease of approximately two percent in $X_{Dol}^{MgCO_3}$ in the composition of the run products relative to the initial analyses. While 006 and 110 *d*-values and intensities should be independent of the ordering state of the dolomite, the intensity of the 015 reflection used by Schultz-Güttler (1986) to measure disorder is a function of both ordering state and composition. An increase in $X_{Dol}^{CaCO_3}$ for dolomites with $X_{Dol}^{CaCO_3} > 0{\cdot}5$ will cause a decrease in the intensity of the ordering reflections, as the presence of Ca on the Mg site will make the structure factors for this site more like those for the Ca site. The size of this effect needs to be evaluated before Schultz-Güttler's results can be accepted.

Despite these criticisms, Schultz-Güttler's results do suggest that the experiments of all previous investigators may represent metastable solvi reflecting variable, metastable ordering states in the dolomite. As the calcite limb of these metastable solvi would lie at higher $X_{Cc}^{MgCO_3}$ values than the stable solvus, all temperatures calculated from calcite–dolomite thermometry may be systematically low.

RE-EVALUATION OF PHASE RELATIONS IN THE SYSTEM $CaCO_3$–$MgCO_3$–$FeCO_3$

Because one or both sets of experimental data on the ternary $CaCO_3$–$MgCO_3$–$FeCO_3$ system must be inaccurate, we are left to create a diagram that will agree with available field and reversed experimental data. Experimental data on the binary systems may be used to constrain these ternary phase relations. Reversed experiments are available for solvi involving calcite–dolomite (Graf & Goldsmith, 1955, 1958; Harker & Tuttle, 1955;

Goldsmith & Heard, 1961; Goldsmith & Newton, 1969; Grummon, 1977; Byrnes & Wyllie, 1981; Fanelli & Wyllie, pers. comm.), calcite-siderite (Goldsmith *et al.*, 1962; Rosenberg, 1963), and magnesite-dolomite (Goldsmith & Heard, 1961; Irving & Wyllie, 1975; Byrnes & Wyllie, 1981). While it is strictly incorrect to use the term 'solvus' to refer to the immiscibility between $R\bar{3}$ and $R\bar{3}/c$ carbonates because of their different structures (*cf.* Reeder, 1983), for brevity we shall refer to these miscibility gaps as 'solvi' in this paper.

$CaCO_3$-$CaMg(CO_3)_2$

The calcite-dolomite join has been experimentally investigated by a number of workers. Because of the relatively rapid reaction rates during experiments, most investigators have assumed that equilibrium was reached during the experiments, which may account for some differences. A best fit for the solvus can be determined by combining reversals from all available experiments. The different starting materials employed may be taken together to provide a single, reversed data set, as Graf & Goldsmith (1958) used magnesian calcite starting material while other workers began with pure calcite, thus constraining the calcite limb of the solvus from both directions.

Powder X-ray diffraction was used for analysis of run-products by all investigators, but different X-ray calibration curves were used. In order to compare the different experiments, they must be referred to the same calibration curve. Bischoff *et al.* (1983) have fit the unit cell parameters of calcites ($X_{Cc}^{MgCO_3}$ = 0·00–0·20) to a smooth curve by a least-squares analysis. Using these data, $d(104)_H$ may be calculated for Mg-calcite solutions and extended to $X_{Cc}^{MgCO_3}$ = 0·5 using several points from Goldsmith *et al.* (1962) (Fig. 2). With this curve and the pressure correction on the position of the solvus given by Goldsmith & Newton (1969), the experimental data have been recalibrated and fit by hand to a single curve at 2 kb (Fig. 3).

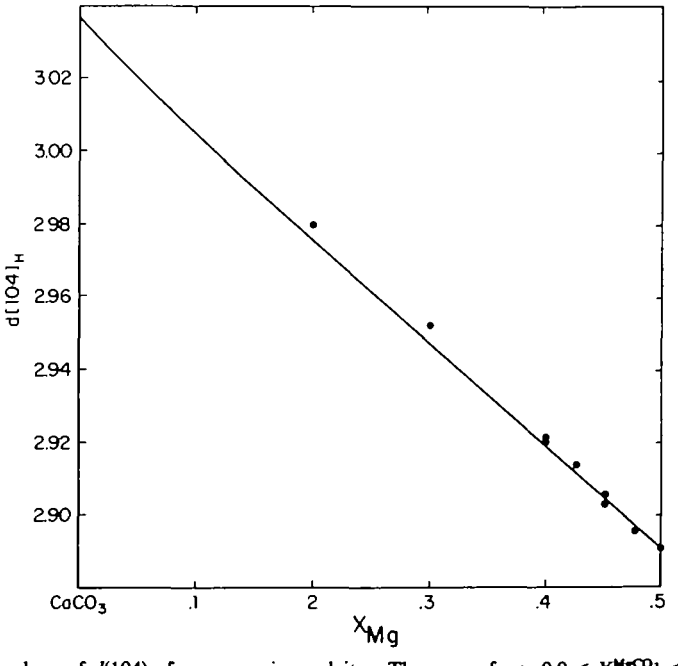

FIG. 2. Calculated values of $d(104)_H$ for magnesian calcites. The curve from 0·0 ≤ $X_{Cc}^{MgCO_3}$ ≤ 0·2 is taken from Bischoff *et al.* (1983). Points at higher values of $X_{Cc}^{MgCO_3}$ are values for disordered carbonates measured by Goldsmith *et al.* (1962), and the curve from 0·2 ≤ $X_{Cc}^{MgCO_3}$ ≤ 0·5 is an extension of the Bischoff *et al.* data fitted to these points.

A caveat is necessary in regard to X-ray determinations of run-product compositions. Because of the fine-grained nature of many run-products, it is often difficult or impossible to obtain compositions using the electron microprobe (Powell *et al.*, 1984). While X-ray *d*-values are sensitive to compositional variations, erroneous results may be obtained if coherent submicroscopic intergrowths have formed. The ideal experiment therefore requires microprobe determination of reversed compositional shifts, as reported by Fanelli & Wyllie (pers. comm.).

It is apparent from Fig. 3 that not all of the experiments can have reached equilibrium. In addition, the solvus is poorly constrained at temperatures < 500 °C. The reversal of Harker & Tuttle (1955) at 600 °C cannot be reconciled with the remainder of the data and was discarded. The reversal of Grummon (1977) at 400 °C requires the calcite limb of the solvus to change slope around 600 °C and has been disregarded. The half-reversal by Goldsmith & Graf (1955, 1958) at 400 °C constrains the solvus at a slightly less Mg-rich position than that

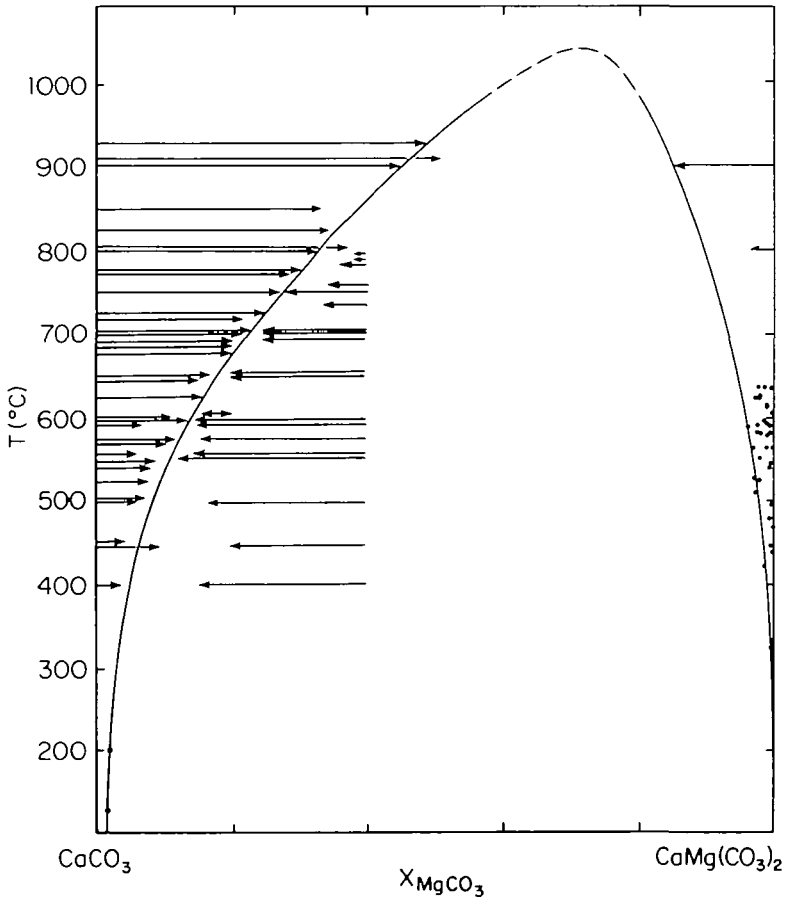

FIG. 3. The calcite-dolomite solvus fit to reversals (Harker & Tuttle, 1955; Graf & Goldsmith, 1958; Goldsmith & Heard, 1961; Goldsmith & Newton, 1969; Grummon, 1977; Byrnes & Wyllie, 1981; Fanelli & Wyllie, pers. comm.). The heads of the arrows show the final compositions, and the direction of the arrow gives the direction of the compositional shift. Experimental pressures corrected to 2 kb using the correction of Goldsmith & Newton (1969). The points near the dolomite limb represent natural dolomite coexisting with calcite analyzed by Sobol (1973), Bowman (1978), Newbitt (1979), Valley (1980), and Treiman & Essene (1983). The two points at low temperatures on the calcite limb are natural calcites whose equilibrium temperatures were estimated from fluid inclusion data by Talantsev (1976).

suggested by Grummon (1977) and agrees with data at 150–200 °C estimated from natural compositions by Talantsev (1976). Likewise, the half-reversals of Harker & Tuttle (1955) at 800 and 900 °C would require a sharp change in the slope of the calcite limb at high temperatures. These data have therefore also been disregarded.

To model the calcite-dolomite solvus thermodynamically it is necessary to estimate the position of the dolomite limb. This has been investigated experimentally by Goldsmith & Heard (1961) and Byrnes & Wyllie (1981). Unfortunately, these experimenters did not use mixtures of calcite and dolomite as starting materials which is requisite for compositional reversals, and these experiments have only limited utility. We have therefore based the location of the dolomite limb of the solvus on the available half-reversals and on compositions of natural dolomites in equilibrium with calcite. Data on dolomite compositions were obtained from Sobol (1973), Bowman (1978), Nesbitt (1979), Bowman & Essene (1982), and Treiman & Essene (1983). Equilibration temperatures were calculated from the calcite limb of the solvus, and the dolomite compositions were used to locate the position of the dolomite limb (Fig. 3). These analyses define a field of dolomite compositions. If each were actually in equilibrium with its coexisting calcite at the temperature shown they should instead fall on the field boundary. The observed scatter may be partially due to analytical error, but the bias of the scatter to low-Ca compositions suggests that many of the dolomites may have reset on cooling to lower temperatures than their coexisting calcites.

$CaCO_3$-$FeCO_3$

Experiments of Rosenberg (1963) and Goldsmith *et al.* (1963) constrain the position of the calcite-siderite solvus. A solvus curve may be fit by hand to the data (Fig. 4). This curve is

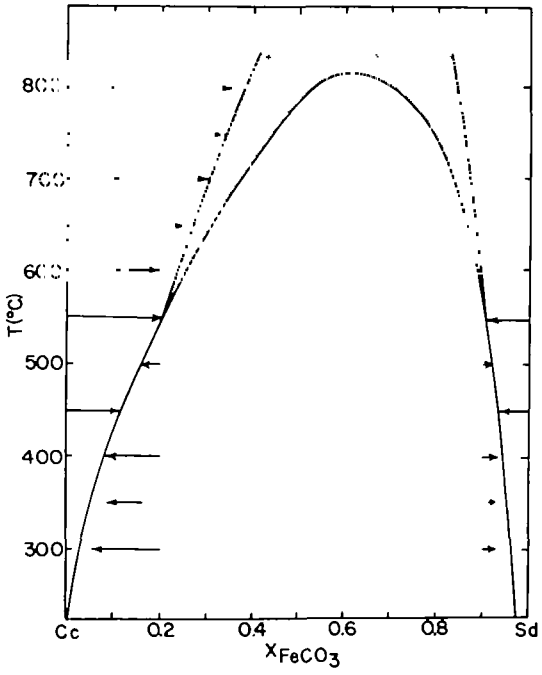

FIG. 4. The calcite-siderite solvus fit to reversals of Goldsmith *et al.* (1962, dots) and Rosenberg (1963*a*, square brackets). The head of the symbol shows the final composition obtained. The shaded field represents the estimated error in extrapolation of the solvus to higher temperatures, suggesting a minimum temperature for the closure of the solvus at ≈ 1100 K as shown.

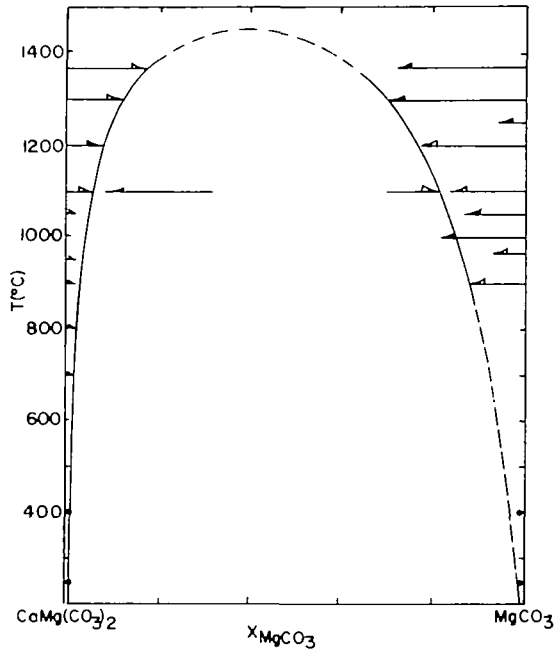

FIG. 5. The magnesite–dolomite solvus fit to available experimental data (Goldsmith & Heard, 1961; Irving & Wyllie, 1975; Byrnes & Wyllie, 1981). The high-temperature section of the solvus is metastable at low pressures relative to incongruent melting reactions.

reasonably well constrained between 325 and 550 °C, but less well located at higher temperatures (Fig. 2).

$CaMg(CO_3)_2$–$MgCO_3$

Three sets of experiments on the magnesite–dolomite join (Goldsmith & Heard, 1961; Irving & Wyllie, 1975; Byrnes & Wyllie, 1981) were used to constrain the location of the solvus down to 1100 °C. At this temperature the dolomite limb is located at $X_{Dol}^{MgCO_3} = 0{\cdot}53$ and the magnesite limb at $X_{Cc}^{MgCO_3} = 0{\cdot}91$. There is little solid-solution along this join at lower temperatures. The position of the solvus remains semi-quantitative because of the lack of compositional reversals at $T < 1100$ °C (Fig. 5). Two analyzed dolomite–magnesite pairs (Frost, 1982; Sanford, 1982) are also shown. While the dolomite compositions agree well with the inferred solvus, the magnesite compositions are slightly subcalcic. This is typical of analyses of carbonates along the magnesite–siderite join, and is discussed in more detail below.

$CaCO_3$–$MgCO_3$–$FeCO_3$

Phase relations in the $CaCO_3$–$MgCO_3$–$FeCO_3$ system may be inferred from natural carbonate assemblages. This approach has several drawbacks. The inevitable variability in the quality of the analyses limits the precision which can be achieved. While obviously inaccurate or poor analyses may be discarded, there is little control over the quality of most of the data. In addition, analyzed pairs may not represent equilibrium assemblages. Unless textural evidence is carefully considered, vein material or other disequilibrium materials may be accidentally analyzed. Substitution of other cations, especially Mn (Essene, 1983) may also occur in metamorphic carbonates. Only carbonates with less than 6 mol per cent

other components have been used in this paper. Re-equilibration during retrograde metamorphism may also be a serious problem.

Even if the analyzed materials represent an equilibrium assemblage, the conditions under which they equilibrated are often poorly defined and much of the precision of an experimental study is lost. Analyses have therefore been grouped into four approximate grades of metamorphism. These are: (1) subgreenschist, $T \sim 250$ °C; (2) biotite grade, $T \sim 400$ °C; (3) amphibolite grade, $T \sim 550$ °C; and (4) granulite grade, $T \sim 700$ °C. The temperature estimates are considered to have a ± 50 °C error. As there are only a few published analyses for the higher temperature facies and the problems of resetting are greatly amplified, the uncertainty in the resulting diagrams is therefore greater.

Figure 1 shows several of the most iron-rich ankerites and siderite/ankerite pairs available from rocks near the biotite isograd. Neither Goldsmith's nor Rosenberg's experiments correctly predicts the maximum amount of $CaFe(CO_3)_2$ possible in natural ankerites. Rosenberg's compositional limit at 500 °C is closer to that suggested by the natural compositions, while Goldsmith's tie-lines more correctly predict the partitioning of Mg/Fe between natural iron rich carbonates.

Figures 6–10 show the analyzed carbonates for each of the grades listed above. Our own data for carbonates from the Michipicoten greenstone belt, Wawa, Ontario are plotted separately for clarity. Two- and three-phase field boundaries have been tentatively located on each diagram. At 400 and 550 °C (greenschist and amphibolite grade respectively) these boundaries have been calculated from ternary activity/composition models (see below). The boundaries in Figs. 6 and 10 have been placed to correspond in form with the theoretical models and Goldsmith *et al.*'s results, and to fit as closely as possible with the binary experimental data and the natural materials.

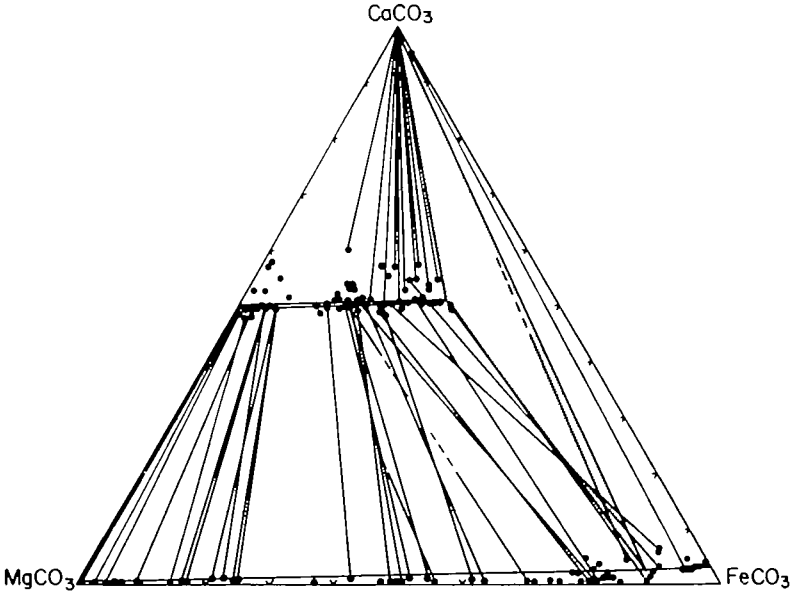

FIG. 6. Carbonates in the system $CaCO_3$-$MgCO_3$-$FeCO_3$ for subgreenschist ($T \approx 250$ °C) conditions. Field boundaries fit graphically and by analogy with calculated 400 and 550 °C results. The three-phase field is stippled. Carbonate analyses renormalized to Ca + Mg + Fe = 1. Data derived from Machamer (1968), Klein (1974, 1978), Pearson (1974), Floran & Papike (1975), Klein & Fink (1976), Lesher (1978), Miyano (1978), Pakkala & Puustinen (1978), Frost (1982), Klein & Gole (1981), and Böhlke (1986). Note apparent metastability of many of the analyzed dolomites.

Comparison of Figs. 6-10 with those of Goldsmith *et al.* (1962) and Rosenberg (1967) shows several significant differences. The calcium content of natural siderites in equilibrium with ankerite is much less than that predicted by the experiments (Klein & Gole, 1981). The calcium content of natural siderites either represents the true equilibrium position of this boundary or the effects of retrograde compositional resetting. Because carbonates are reactive, they may reset on cooling more rapidly than silicates. Exsolution textures are commonly reported in rhombohedral carbonates (Harker & Tuttle, 1955; Ackermand & Morteani, 1972; Perkins *et al.*, 1982; Wada & Suzuki, 1983), and such textures should be sought in calcian siderites, though exsolution may be so rapid that lamellae are preserved only under special circumstances.

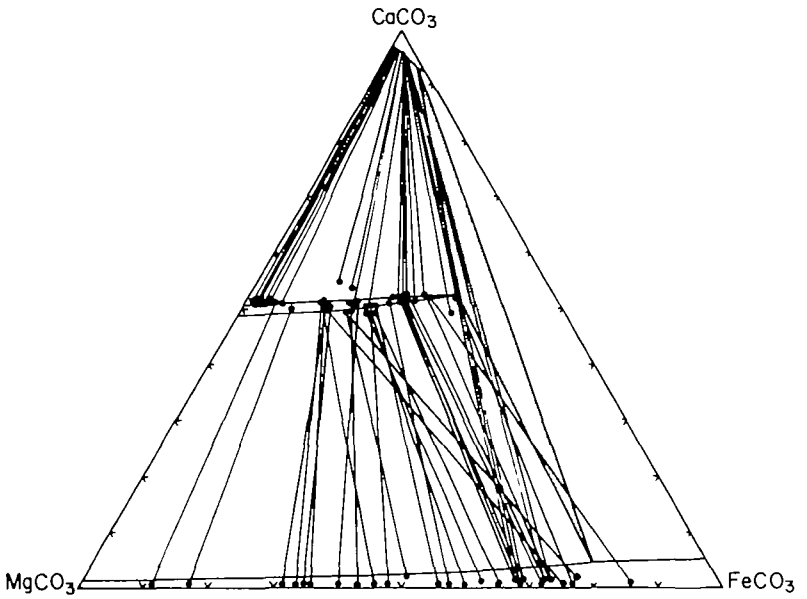

FIG. 7. Carbonates in the system $CaCO_3$-$MgCO_3$-$FeCO_3$ for biotite grade ($T \approx 400$ °C) conditions Field boundaries calculated from the solution model. Data derived from Pinsent & Smith (1975), Talantsev (1978), Talantsev & Sazonov (1979), Haase (1979), Sanford (1982), and Dietrich (1983).

The subgreenschist and biotite grade diagrams show crossing tie-lines, which may be due to temperature variations within each group, analytical inaccuracies, and/or analysis of disequilibrium pairs. Where the tie-lines cross at large angles, analysis of disequilibrium pairs is likely. This initially occurred with some of our own Wawa analyses when material from a veinlet was plotted with matrix materials.

Assemblages analyzed by Pinsent & Smith (1975) suggest that the three-phase carbonate field for the biotite zone is shifted to more Mg-rich conditions than suggested by other workers, while the K_D for their siderite-ankerite pairs agrees with other anlyses. The calcites analyzed by Pinsent & Smith may not have equilibrated with the siderite and ankerite but this cannot be determined without careful examination of the analyzed samples.

Due to the scarcity of data, the diagrams for the amphibolite and granulite facies are largely schematic and their general form has been made to conform to that of Goldsmith *et al.* (1962). On the granulite diagram a single calcite analysis, reported to coexist with an unanalyzed siderite (Butler, 1969), falls well within the inferred one-phase field for calcite

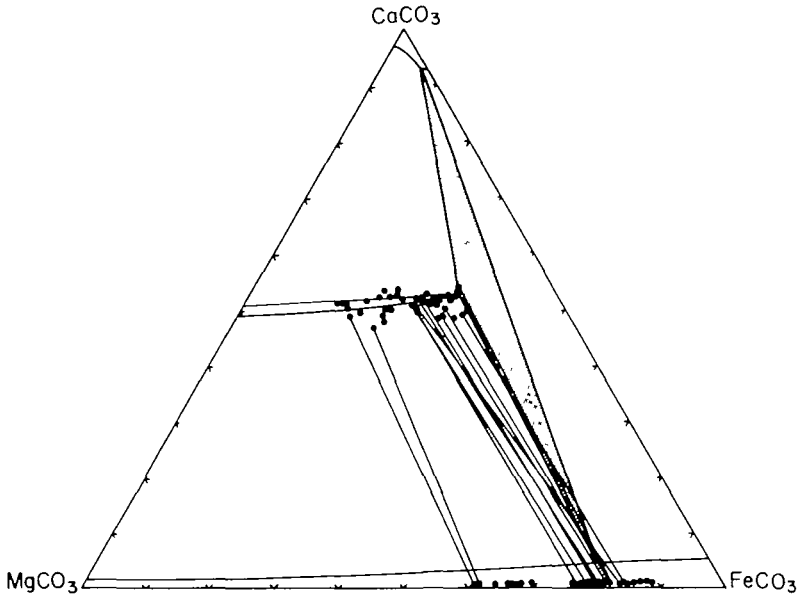

FIG. 8. Carbonates in the system $CaCO_3$-$MgCO_3$-$FeCO_3$ from the Michipicoten Iron-Range, Wawa, Ontario. The fields shown are the same as in Fig. 7. Note apparent metastability of some of the analyzed dolomites.

(Fig. 10). The calcite may have originally equilibrated with siderite but later reset its composition at lower temperatures, or it may not have equilibrated with siderite at the peak of metamorphism and the siderite now present may have exsolved or recrystallized during retrograde re-equilibration.

ACTIVITY-COMPOSITION RELATIONS IN THE SYSTEM $CaCO_3$-$MgCO_3$-$FeCO_3$

We may use these derived phase diagrams for the system $CaCO_3$-$MgCO_3$-$FeCO_3$ to model approximate activity/composition relations for this system. Such relations for calcite-structure carbonates on the join $CaCO_3$-$MgCO_3$ have previously been derived by Gordon & Greenwood (1970) and Skippen (1974). We have remodeled activity/composition relations on this join using the newer experiments on the calcite–dolomite and magnesite–dolomite solvi (Figs. 4 and 5). With the exception of calculations by Bickle & Powell (1977) in which only the calcite half of the calcite–siderite solvus was modeled, mixing models for other joins in this system are unavailable.

In any system, solution modeling requires solving one equation of the form:

$$\mu_\alpha^{0,i} - \mu_\beta^{0,i} = \Delta\mu_{\alpha-\beta}^{0,i} = RT\ln(X_\beta^i/X_\alpha^i) + RT\ln\gamma_\beta^i - RT\ln\gamma_\alpha^i, \quad (6)$$

for each of the components considered, where the superscript refers to the ith component, the subscript to the phase, X_α^i and X_β^i are the compositions of the two phases on the solvus, and $\Delta\mu_{\alpha-\beta}^{0,i}$ is the difference in the standard state chemical potential between the two phases for the ith component. Calcite, magnesite and siderite are assumed to represent the end-member phases of a single type of solution, while dolomite-structure carbonates represent a second solution type. There are thus two sets of mixing parameters, one for calcite-structure carbonates and one for dolomite-structure carbonates.

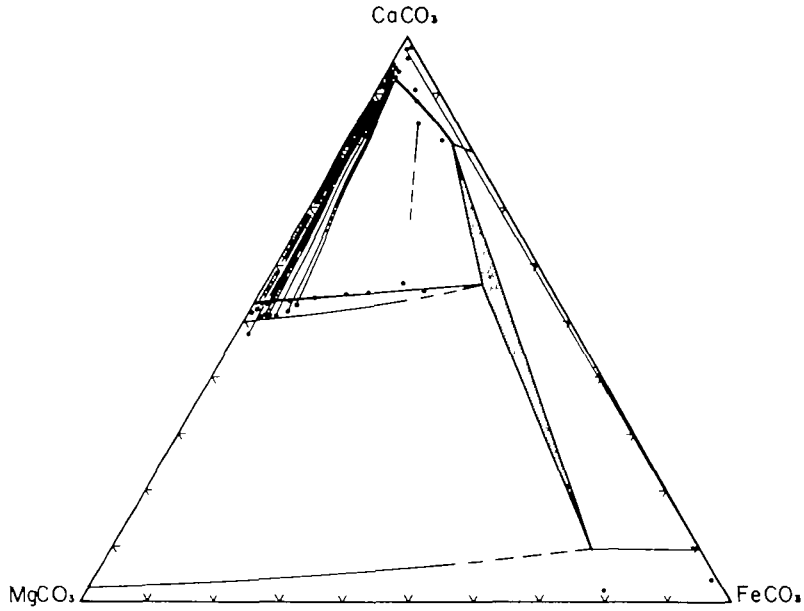

FIG. 9. Carbonates in the system $CaCO_3$-$MgCO_3$-$FeCO_3$ for amphibolite grade conditions ($T \approx 550$ °C). Field boundaries calculated from the solution model. Data derived from Klein (1966, 1978), Floran & Papike (1978), Hall (1980), and Sanford (1982).

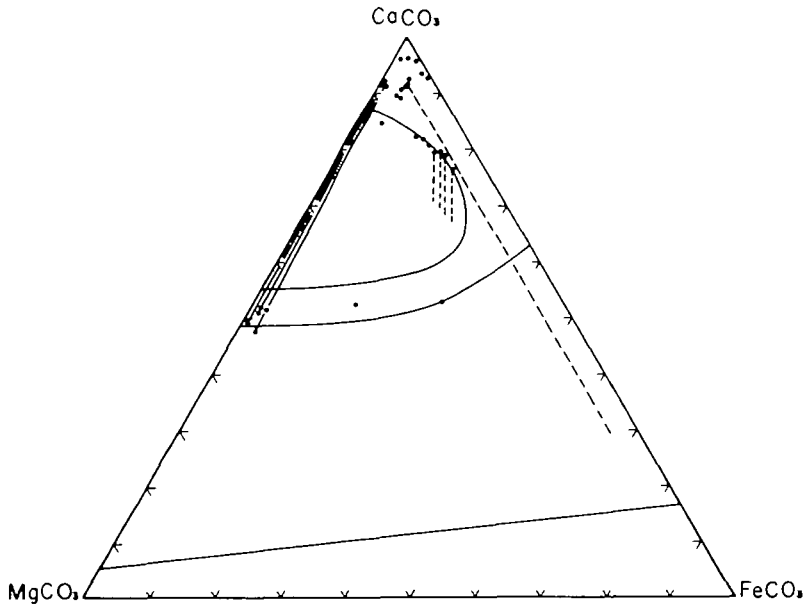

FIG. 10. Carbonates in the system $CaCO_3$-$MgCO_3$-$FeCO_3$ for granulite grade conditions ($T \approx 700$ °C). Field boundaries fit graphically and by analogy with the calculated 400 and 550 °C results and those of Goldsmith *et al.* (1962). Data derived from Butler (1969), Shibuya & Harada (1976), and Klein (1978). Tie-line for a calcite–siderite (siderite unanalyzed) pair (Butler, 1969) is shown.

The ternary subregular two-phase model used here considers macroscopic thermodynamic properties. Models by Navrotsky & Loucks (1977) and Burton & Kikuchi (1984) have attempted to incorporate microstructural considerations. As has previously been noted by Holland *et al.* (1980) with respect to the analogous enstatite–diopside system, a macroscopic model is a reasonable choice when the object is to reproduce the phase diagram. Indeed, the microscopic models presently available have so far failed in this regard in all but the most qualitative sense. While it might be possible to incorporate cooperative disordering (Navrotsky & Loucks, 1977), accurate data on ordering states for ternary carbonates are required (Davidson, 1984), but few quantitative data exist (Goldsmith & Heard, 1961; Beran & Zeeman, 1977; Reeder & Nakajima, 1982; Reeder, 1983; Reeder & Wenk, 1983). As the position of the solvus must reflect the ordering state, such disordering as occurs in the temperature range modeled must be implicit in the macroscopic model. An accurate explicit model must await the availability of sufficient ordering data.

For ternary systems, a subregular two-phase mixing model requires knowledge of 17 mixing parameters; including six binary Margules coefficients (W) and a ternary coefficient (C) for each of the two phases, and the difference in standard state chemical potential ($\Delta\mu^0$) between the two phases at each of the three end-member compositions (Saxena, 1973). Values for most of these parameters may be obtained by modeling the binary phase relations presented above.

At a given temperature, the calcite–siderite solvus may be represented by the equations:

$$\Delta\mu^{0,\,CaCO_3}_{Cc-Sd} = 0 = RT\ln\left(\frac{X^{CaCO_3}_{Sd}}{X^{CaCO}_{Cc}}\right)+(X^{FeCO_3}_{Sd})^2(W^{CaFe}_{Cc}+ 2X^{CaCO_3}_{Sd}(W^{FeCa}_{Cc}-W^{CaFe}_{Cc}))-(X^{FeCO_3}_{Cc})^2(W^{CaFe}_{Cc}+2X^{CaCO_3}_{Cc}(W^{FeCa}_{Cc}-W^{CaFe}_{Cc})) \quad (7)$$

$$\Delta\mu^{0,\,FeCO_3}_{Cc-Sd} = 0 = RT\ln\left(\frac{X^{FeCO_3}_{Sd}}{X^{FeCO_3}_{Cc}}\right)+(X^{CaCO_3}_{Sd})^2(W^{FeCa}_{Cc}+ 2X^{FeCO_3}_{Sd}(W^{CaFe}_{Cc}-W^{FeCa}_{Cc}))-(X^{CaCO_3}_{Cc})^2(W^{FeCa}_{Cc}+2X^{FeCO_3}_{Cc}(W^{CaFe}_{Cc}-W^{FeCa}_{Cc})), \quad (8)$$

where $\Delta\mu^{0,\,i}_{Cc-Sd}$ is equal to $\Delta\mu^{0,\,i}_{Cc}-\Delta\mu^{0,\,i}_{Sd}$ for the ith component. These equations may be solved simultaneously for the two unknown Margules coefficients. Because end-member ankerite is unstable, calculations on the $CaCO_3$–$FeCO_3$ binary cannot be used to obtain W^{CaFe}_{Dol} and W^{FeCa}_{Dol}. Resultant values for calcite-structure carbonates obtained from the solvus shown in Fig. 4 between 573 and 1073 K have been fit to curvilinear equations:

$$W^{CaFe}_{Cc} = 27313{\cdot}2-5{\cdot}79651\times10^6/T-1{\cdot}43147\times10^{-3}T^2\ (\pm5{\cdot}0\ \mathrm{J}\ T,\ \mathrm{K}), \quad (9)$$

$$W^{FeCa}_{Cc} = -70751{\cdot}4+91{\cdot}8848T+2{\cdot}79244\times10^7/T-3{\cdot}59552\times10^{-2}T^2\ (\pm2{\cdot}1\ \mathrm{J}\ T,\ \mathrm{K}). \quad (10)$$

Curvilinear functions for the variations in Margules parameters with temperature are more complex than the linear functions commonly presented (Saxena, 1973; Lindsley *et al.*, 1981). However, a linear model would introduce unnecessary errors, as the data show a distinct curvature. Unfortunately, equations of this type extrapolate poorly, and use of this model outside of the fitted range is questionable.

Two solvi exist on the join $CaCO_3$–$MgCO_3$: calcite–dolomite and magnesite–dolomite. Lindsley *et al.* (1981) noted that use of Margules equations to independently model either section of a compound binary leaves the intermediate phase metastable when the whole join is considered. In the case of the calcite–dolomite–magnesite join such a model leaves dolomite metastable relative to four potential assemblages: calcian dolomite–magnesite,

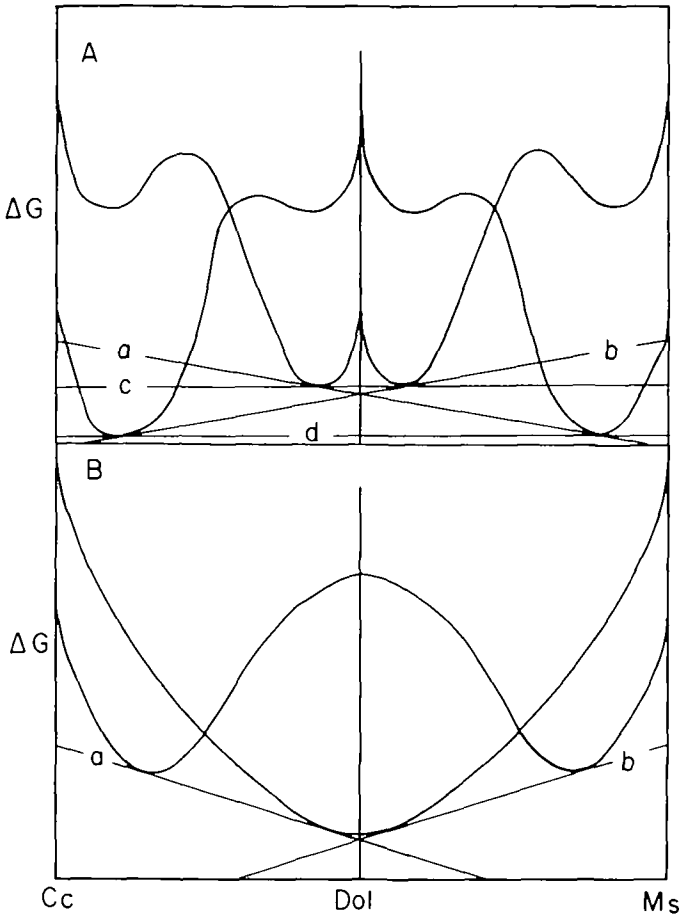

FIG. 11. Schematic Gibbs' energy composition relations for the system $CaCO_3$–$MgCO_3$. (A) The Gibbs' energy curves that result from independent modeling of the dolomite–calcite and dolomite–magnesite joins. Solvi between (a) mineral pairs calcian dolomite–magnesite, (b) magnesian dolomite–calcite, (c) calcian dolomite–magnesian dolomite, and (d) magnesian calcite–calcian magnesite are all more stable than dolomite of composition $CaMg(CO_3)_2$. (B) The Gibbs' energy curves as modeled. Dolomite of composition $CaMg(CO_3)_2$ remains stable, (a) calcite–dolomite solvus, and (b) magnesite–dolomite solvus.

magnesian dolomite–calcite, magnesian dolomite–calcian dolomite, or magnesian calcite–calcian magnesite (Fig. 11A). This may be avoided by treating the entire join as a unit, assuming that $R\bar{3}$ and $R\bar{3}/c$ carbonates are treated as separate solutions (Fig. 11B). The form of the G/X curves generated by this approach is similar to that suggested by Carpenter & Putnis (1985).

At a given temperature, the equations:

$$\Delta\mu^{0,\,MgCO_3}_{Dol\text{–}Cc} = RT\ln\left(\frac{X^{MgCO_3}_{Cc}}{X^{MgCO_3}_{Dol}}\right) + (X^{CaCO_3}_{Cc})^2(W^{MgCa}_{Cc} + 2X^{MgCO_3}_{Cc}(W^{CaMg}_{Cc} - W^{MgCa}_{Cc})) - (X^{CaCO_3}_{Dol})^2(W^{MgCa}_{Dol} + 2X^{MgCO_3}_{Dol}(W^{CaMg}_{Dol} - W^{MgCa}_{Dol})), \quad (11)$$

$$\Delta\mu^{0,\,CaCO_3}_{Dol\text{–}Cc} = RT\ln\left(\frac{C^{CaCO_3}_{Cc}}{X^{CaCO_3}_{Dol}}\right) + (X^{MgCO_3}_{Cc})^2(W^{CaMg}_{Cc} + 2X^{CaCO_3}_{Cc}(W^{MgCa}_{Cc} - W^{CaMg}_{Cc})) - (X^{MgCO_3}_{Dol})^2(W^{CaMg}_{Dol} + 2X^{CaCO_3}_{Dol}(W^{MgCa}_{Dol} - W^{CaMg}_{Dol})) \quad (12)$$

must be simultaneously satisfied for both the calcite–dolomite and magnesite–dolomite solvi. An additional constraint may be placed on the result by requiring that calcite and magnesite remain stable for the compositions $CaCO_3$ and $MgCO_3$. The standard state chemical potential ($\Delta\mu^0$) terms as written must therefore remain positive.

Margules coefficients were allowed to vary with temperature as:

$$W_G = W_H - TW_S. \tag{13}$$

and the Gibbs' energy of the reaction Dolomite = Calcite + Magnesite was forced to fit the known values (Robie *et al.*, 1978) as a function of temperature. The Gibbs' energy of dolomite is calculated as:

$$\Delta G_{Dol}^{(CaMg)CO_3} = (\mu_{Dol}^{0,\,CaCO_3} + \mu_{Dol}^{0,\,MgCO_3})/2 + RT\Sigma X^i \ln X^i + RT\Sigma X^i \ln \gamma^i, \tag{14}$$

where the chemical potentials are those for end-member compositions taken as the standard state. This value can be the Gibbs' energy of formation from the elements or the oxides depending on the values chosen for the μ^0 terms.

The resulting system of five equations was solved by linear regression using the MIDAS statistical package available at the University of Michigan. During the course of the refinement the solution was found to be relatively insensitive to the magnitude of the $\Delta\mu^0$ terms, which were therefore arbitrarily fixed at 20·92 kJ (5·0 kcal) (Table 2).

No attempt was made to adjust the model by minimizing the residuals to the data points (cf. Lindsley *et al.*, 1981), because there is an equal probability that any point within a reversal lies on the reaction in question and any reasonable curve within the reversal brackets is

TABLE 2

Mixing parameters for carbonates in the system $CaCO_3$-$MgCO_3$-$FeCO_3$. All values in J mol^{-1}

	Structure type	
Coefficient	*Calcite*	*Dolomite*
W_H^{CaMg}	23240·0	−96850·0
W_S^{CaMg}	0·0	−36·23
W_H^{MgCa}	24300·0	−55480·0
W_S^{MgCa}	7·743	22·850
W_H^{MgFe}	0	0
W_H^{FeMg}	0	0
W_H^{CaFe}	*	−1040·0
W_{S1}^{CaFe}	*	212·4
W_{S2}^{CaFe}	0	−0·2027
W_H^{FeCa}	*	−86740·0
W_{S1}^{FeCa}	*	−71·18
W_{S2}^{FeCa}	0	0·09184
C_H	see equation 18	−185450·0
C_{S1}		369·2
C_{S2}		−0·1418

$\Delta\mu_{Dol-Cc}^{0,\,CaCO_3} = \mu_{Dol}^{0,\,CaCO_3} - \mu_{Cc}^{0,\,CaCO_3} = 20920{\cdot}0$

$\Delta\mu_{Dol-Cc}^{0,\,MgCO_3} = \mu_{Dol}^{0,\,MgCO_3} - \mu_{Cc}^{0,\,MgCO_3} = 20920{\cdot}0$

$\Delta\mu_{Dol-Cc}^{0,\,FeCO_3} = \mu_{Dol}^{0,\,FeCO_3} - \mu_{Cc}^{0,\,FeCO_3} = 20920{\cdot}0$

* See equations (9) and (10).

equally likely to represent the true position of the reaction. Minimizing the residuals to the experimental results in such a case implies the possibly erroneous assumption that the experimental results represent equilibrium values rather than limits on the position of the actual equilibrium. In situations where graphically drawn boundaries which may be in agreement with data at one pressure or temperature disagree with results extrapolated from other P/T conditions a more complex model may be necessary to obtain a result in reasonable agreement with the bulk of the data (Lindsley *et al.*, 1981).

The formulation used here for dolomite solid solutions treats dolomites as falling on a hypothetical ordered $CaCO_3$–ordered $MgCO_3$ join. Unfortunately, the equations thus do not directly generate activities for end-member dolomite. These can be derived by writing equation (14) for the entire join and for either the calcite-dolomite or dolomite-magnesite subjoin. As the total Gibbs energy must be the same the two equations can be set equal and solved for $RT\ln\gamma_{Dol}^{(Ca,Mg)CO_3}$. This yields:

$$RT\ln\gamma_{Dol}^{(Ca,Mg)CO_3} = (1/X_{Dol}^{(Ca,Mg)CO_3})[X_{Dol}^{MgCO_3}\cdot\mu_{Dol}^{0,\,MgCO_3} - X_{Dol}^{(Ca,Mg)CO_3}\cdot\mu_{Dol}^{0,\,(Ca,Mg)CO_3} - X_{Dol}^{CaCO_3}\cdot\mu_{Dol}^{0,\,CaCO_3} + RT(\ln(X_{Dol}^{MgCO_3}\cdot\gamma_{Dol}^{MgCO_3}) - \ln(X_{Dol}^{(Ca,Mg)CO_3}\cdot\gamma_{Dol}^{(Ca,Mg)CO_3}) - X_{Dol}^{CaCO_3}\cdot\ln(X_{Dol}^{CaCO_3}\cdot\gamma_{Dol}^{CaCO_3}) - 2X_{Dol}^{CaCO_3}\cdot\ln 2)] \quad (15)$$

for the calcite-dolomite join, and:

$$RT\ln\gamma_{Dol}^{(Ca,Mg)CO_3} = (1/X_{Dol}^{(Ca,Mg)CO_3})[X_{Dol}^{CaCO_3}\cdot\mu_{Dol}^{0,\,CaCO_3} - X_{Dol}^{(Ca,Mg)CO_3}\cdot\mu_{Dol}^{0,\,(Ca,Mg)CO_3} - X_{Dol}^{CaCO_3}\cdot\mu_{Dol}^{0,\,CaCO_3} + RT(\ln(X_{Dol}^{CaCO_3}\cdot\gamma_{Dol}^{CaCO_3}) - \ln(X_{Dol}^{(Ca,Mg)CO_3}\cdot\gamma_{Dol}^{(Ca,Mg)CO_3}) - X_{Dol}^{MgCO_3}\cdot\ln(X_{Dol}^{MgCO_3}\cdot\gamma_{Dol}^{MgCO_3}) - 2X_{Dol}^{MgCO_3}\cdot\ln 2)] \quad (16)$$

for the dolomite-magnesite join. The values of the μ^0 may be calculated from data in Robie *et al.* (1978) for calcite and magnesite and the $\Delta\mu^0$ terms in Table 3. An alternative approach to this problem has been taken by Davidson (1984). By analogy with her derivation for diopside, the chemical potential of dolomite may be taken as the average of the chemical potentials of ordered $CaCO_3$ and ordered $MgCO_3$.

TABLE 3

Coefficients and statistical data for equations (23) and (31). R^2 *and standard error values given separately for the* $MgCO_3$ *and* $FeCO_3$ *sections of the equation. Significance factor* (σ) *shows the probability that the value of the coefficient is zero*

Coefficient	*Value*	*S.E.*	σ
A	−2360·0	968·0	0·024
B	−0·01345	0·00225	0·000
C	2620·0	1404·0	0·077
D	2608·0	412·0	0·000
E	334·0	47·0	0·000
R^2 = 0·99893			
S.E. of the estimate for binary $CaCO_3$–$MgCO_3$ compositions = 7·1254			
a	1718·0	187·0	0·000
b	−10610·0	532·0	0·000
c	22·49	1·97	0·000
d	−26260·0	2940·0	0·000
e	1·333	0·079	0·000
f	$0{\cdot}32837\times10^7$	$0{\cdot}18406\times10^6$	0·000
R^2 = 0·99884			
S.E. of the estimate for ternary compositions = 7·9311			

In order to extend this analysis to the ternary, the following coefficients must be obtained: $\Delta\mu^{0,\,FeCO_3}_{Dol-Cc}$, W^{CaFe}_{Dol}, W^{FeCa}_{Dol}, W^{FeMg}_{Cc}, W^{MgFe}_{Cc}, W^{FeMg}_{Dol}, W^{MgFe}_{Dol}, and the ternary coefficients C_{Cc} and C_{Dol}. No solvus is known on the join $MgCO_3$-$FeCO_3$ down to 250 °C. Assuming a regular solution model, a maximum value for W^{MgFe}_{Cc} ($= W^{FeMg}_{Cc}$) may be calculated as (Saxena, 1973):

$$2RT_C = W, \tag{17}$$

where R is the gas constant and T_C is the temperature at the crest of the solvus. This analysis yields a maximum value of 8·8 kJ for W^{MgFe}_{Cc}. For the purposes of this paper, $W^{MgFe}_{Cc} = W^{FeMg}_{Cc}$ and $W^{MgFe}_{Dol} = W^{FeMg}_{Dol}$ are both assumed to equal zero.

Following Ganguly & Saxena (1984) the ternary coefficients may be estimated using the method of Wohl (1953)

$$C = ((W^{21} - W^{12}) + (W^{13} - W^{31}) + (W^{32} - W^{23}))/2. \tag{18}$$

This equation yields the magnitude but not the sign of the ternary coefficients; the sign will change with an arbitrary renumbering of the components. Our calculations showed that a negative sign was appropriate for calcite-structure solutions. The value of $\Delta\mu^{FeCO_3}_{Dol-Cc}$ was arbitrarily set to 20·92 kJ (5·0 kcal) by analogy with the $CaCO_3$-$MgCO_3$ join.

Because of the poorly constrained nature of our knowledge of ternary tie-lines, regression techniques could not be used to determine the values of the remaining parameters. Instead, reasonable choices were made for the position of the siderite corner of the three phase field consistent with the calcite–siderite–magnesite solvus and the ankerite-siderite K_D (see Fig. 15). The ankerite-siderite tie line was then used to directly calculate values for W^{CaFe}_{Dol}, W^{FeCa}_{Dol}, and C_{Dol} at 250, 400, and 500 °C. The resultant values were not linear functions of temperature, and have been fit to equations of the form (Table 2):

$$W_G(\text{or } C_G) = W_H - T(W_{S1} + W_{S2}\,T)\ (T, K). \tag{22}$$

The resultant field boundaries are shown on Figs. 6–9. No attempt was made to model the 700 °C solvus, as the continuous one-phase field from dolomite to calcite suggests that dolomites become progressively disordered as their iron content increases.

In areas of the ternary where only calcite-type structures are stable (near the $CaCO_3$-$FeCO_3$ join) tie-lines were calculated using the TERNGAP program (Saxena, 1973). A simple modification of subroutine BIGAP to accept two solution types in calculations of binary solvi proved successful, but the Newton-Raphson technique in BIGAP and TERNGAP did not converge for our ternary compositions. A secant-type solution method was therefore employed for ternary calculations to solve equations (19–21) (Appendix 1) for three compositional variables. The fourth independent compositional variable is arbitrarily fixed for individual calculations and then incremented in order to obtain a range of tie-lines across the ternary. This program did not successfully calculate the dolomite-ankerite-magnesite solvus at 250 °C and the high-iron end of the siderite-dolomite solvus at 550 °C (dashed region, Fig. 14). The 250 °C solvus was estimated using the value of K_D from the three-phase field assuming that the phase boundaries are linear between the three-phase field and the dolomite-magnesite join at this temperature. The calculated phase diagrams for 250, 400, and 550 °C, including calculated tie-lines are shown in Figs. 12–14.

The coefficients presented in this study are subject to several temperature restrictions. The $CaCO_3$-$MgCO_3$ and $CaCO_3$-$FeCO_3$ binaries were fit at 250–900 °C and 250–800 °C respectively, and values for W^{CaFe}_{Dol} and W^{FeCa}_{Dol} are given as fits to the three calculated data points (250, 400, and 550 °C). The models should not be used beyond these temperature ranges.

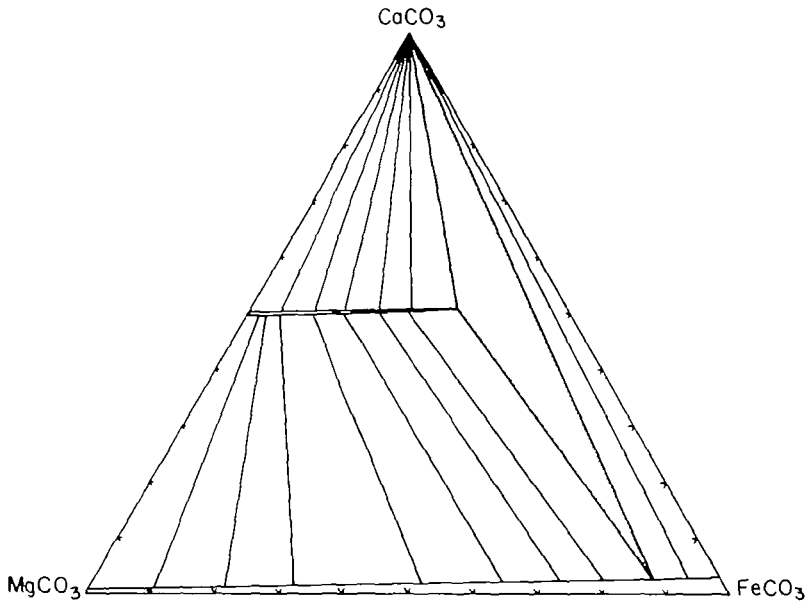

FIG. 12. Thermodynamically calculated phase diagram with tie-lines for the system $CaCO_3$-$MgCO_3$-$FeCO_3$ at 250 °C. Field boundaries and tie-lines generated using a ternary activity model or calculated K_D from three-phase field.

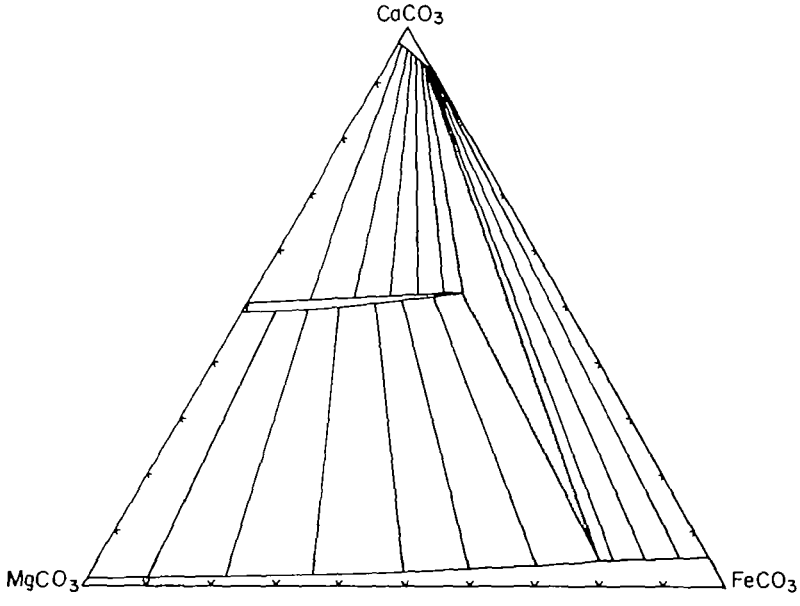

FIG. 13. Thermodynamically calculated phase diagram with tie-lines for the system $CaCO_3$-$MgCO_3$-$FeCO_3$ at 400 °C. Field boundaries and tie-lines generated using a ternary activity model.

CARBONATE THERMOMETRY

Calcite–dolomite thermometry

Calcite–dolomite thermometry has been widely applied (e.g., Goldsmith & Graf, 1958; Hatcher *et al.*, 1973; Hutcheon & Moore, 1973; Sobol, 1973; Puhan, 1976; Rice, 1977; Suzuki, 1977; Kretz, 1980; Bowman & Essene, 1982; Nesbitt & Essene, 1982; Perkins *et al.*, 1982; Wada & Suzuki, 1983) since it was first suggested by Harker & Tuttle (1955) and by Graf & Goldsmith (1955). The position of the solvus is now reasonably well known (± 10 °C) between 500 and 800 °C (Fig. 4). Outside of this range the reversal brackets widen and potential errors are rapidly increased.

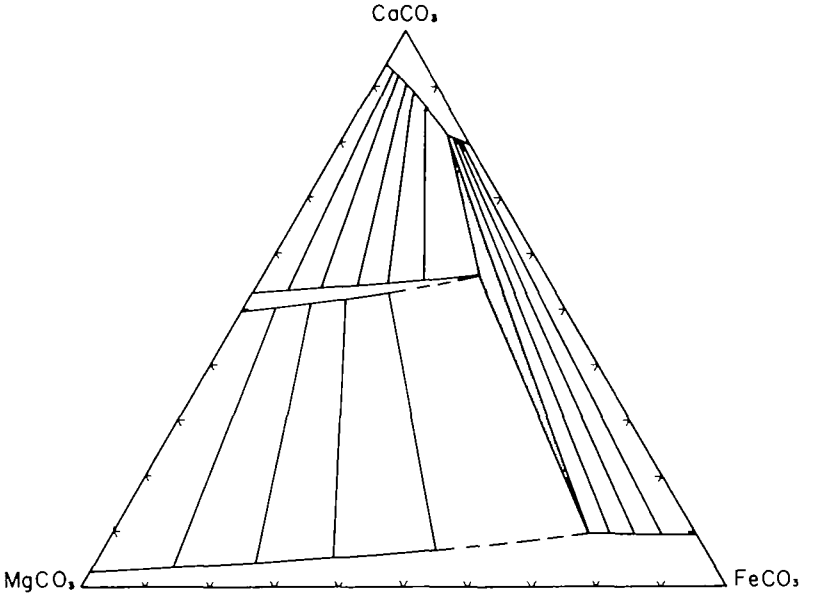

FIG. 14. Thermodynamically calculated phase diagram with tie-lines for the system $CaCO_3$-$MgCO_3$-$FeCO_3$ at 550 °C. Field boundaries and tie-lines generated using a ternary activity model.

The most recent experimental calibration of the calcite–dolomite solvus (Goldsmith & Newton, 1969) is similar to ours. The mole fraction of $MgCO_3$ in calcite as a function of temperature along the solvus may be fit to an equation of the form:

$$T = A(X_{Cc}^{MgCO_3}) + B/(X_{Cc}^{MgCO_3})^2 + C(X_{Cc}^{MgCO_3})^2 + D(X_{Cc}^{MgCO_3})^{0.5} + E \ (T, \mathrm{K}). \qquad (23)$$

A least-squares fit to this equation was obtained in the range 473–1173 K based on the solvus shown (Fig. 3) using the MIDAS package. The parameters are listed in Table 3.

Barron (1974), Talantsev (1976, 1978), and Bickle & Powell (1977) have evaluated the effect of $FeCO_3$ on calcite–dolomite thermometry. Models proposed by Barron (1974) and Talantsev (1976, 1978) were based on the experiments of Rosenberg (1967) and Goldsmith *et al.* (1962). As the details of one of both of these experiments are incorrect, these models must contain errors. Bickle & Powell (1977) assumed that calcite activity relations can be described by symmetrical calcite–siderite and calcite–dolomite models (though both solvi are distinctly asymmetrical). Assuming $W^{MgFe} = 0$ and treating all carbonates ($R\bar{3}$ and $R\bar{3}/c$) as a single

solution type with Margules' parameters W^{ij} (no subscript), the ternary regular solution equations are:

$$-\Delta G = 0 = RT\ln\left(\frac{X_{Cc}^{CaCO_3}\cdot X_{Cc}^{MgCO_3}}{X_{Dol(M2)}^{CaCO_3}\cdot X_{Dol(M1)}^{MgCO_3}}\right)+ W^{CaMg}\cdot(1-X_{Cc}^{FeCO_3}-2X_{Cc}^{MgCO_3}\cdot X_{Cc}^{CaCO_3})+W^{CaFe}\cdot X_{Cc}^{FeCO_3}\cdot(1-2X_{Cc}^{CaCO_3}), \quad (24)$$

$$-\Delta G = 0 = RT\ln\left(\frac{X_{Cc}^{CaCO_3}\cdot X_{Cc}^{FeCO_3}}{X_{Dol(M2)}^{CaCO_3}\cdot X_{Dol(M1)}^{FeCO_3}}\right)+ W^{CaFe}\cdot(1-X_{Cc}^{MgCO_3}-2X_{Cc}^{FeCO_3}\cdot X_{Cc}^{CaCO_3})+W^{CaMg}\cdot X_{Cc}^{MgCO_3}\cdot(1-2X_{Cc}^{CaCO_3}). \quad (25)$$

Equation (25) has been slightly modified from their equation (4) to correct a typographical error. Bickle & Powell further simplified these equations by assuming $X_{Cc}^{FeCO_3}$ and $X_{Cc}^{MgCO_3}$ are small (< 4 mol per cent). Alternatively, subtracting (24) from (25) yields the simple equation:

$$-\Delta G = 0 = RT\ln\left(\frac{X_{Cc}^{MgCO_3}\cdot X_{Dol(M1)}^{FeCO_3}}{X_{Cc}^{FeCO_3}\cdot X_{Dol(M1)}^{MgCO_3}}\right)+(W^{CaMg}-W^{CaFe})\cdot X_{Cc}^{CaCO}. \quad (26)$$

If we examine:

$$K_{D,\,Ank/Cc} = (X^{Fe}/X^{Ca})_{Ank}/(X^{Fe}/X^{Ca})_{Cc}, \quad (27)$$

as calculated from natural assemblages, these values are rather scattered at lower temperatures but around 400 °C the data are more closely constrained, and give $K_D = 15 \pm 5$. Equation (27) relates the calcium content of the dolomite to its iron content given a calcite composition. A third relation is generated as:

$$X_{Dol}^{CaCO_3}+X_{Dol}^{MgCO_3}+X_{Dol}^{FeCO_3} = 1. \quad (28)$$

Equations (23–25) allow calculation of the dolomite/ankerite limb of the solvus given the position of the calcite limb. Unfortunately, neither approach reproduces the observed phase relations for $X_{Dol}^{FeCO_3} > 3$ per cent, and Bickle & Powell's calibration cannot be used for most ternary carbonates.

There are two alternative approaches to calcite–ankerite thermometry. A plot of K_D:

$$K_{D,\,Ank/Cc} = (X^{Fe}/X^{Mg})_{Ank}/(X^{Fe}/X^{Mg})_{Cc}, \quad (29)$$

vs. temperature illustrates the change of the calcite–ankerite tie-lines with temperature. If the temperatures at which a series of carbonate pairs equilibrated are known, a plot of K_D vs. T may be useful for thermometry (Bickle & Powell, 1977), allowing calculation of a more accurate thermometer directly from the solution models presented above. Such a thermometer is sensitive to errors due to compositional resetting of individual phases, as changes in the composition of either phase would change the calculations. The relatively small proportions of $FeCO_3$ present in dolomite and $(Fe,Mg)CO_3$ in calcite magnify the errors.

Equations (19–21) may be solved directly for temperature after factoring out the temperature dependencies of the Margules parameters (equation 13). For equation (19) we derive:

$$\frac{\Delta\mu_{Dol-Cc}^{CaCO_3}-W_{H,Cc}+W_{H,Dol}}{R\ln\left(\frac{X_{Cc}^{CaCO_3}}{X_{Dol}^{CaCO_3}}\right)-W_{S,Cc}+W_{S,Dol}} = T\,(\mathrm{K}). \quad (30)$$

In this equation the W_H terms may be calculated by inserting W_H for the Margules coefficients in the $RT\ln\gamma$ sections of equation (19) (cf. equation 14). The W_S terms are derived similarly. The temperature dependence of the ternary coefficient (C) implicit in both the W_H and W_S terms is obtained by splitting it into its component Margules parameters following equation (18).

A second approach to thermometry in the ternary system utilizes the width of the solvus as the thermometer. Each member of the carbonate pair may be used to yield a separate temperature. The temperature obtained is less sensitive to resetting of one phase or to minor inaccuracies in the analyses. A ternary thermometer may be obtained from our data by expanding (23) as follows:

$$T^{FeMg} = T^{Mg} + a(X_{Cc}^{FeCO_3}) + b(X_{Cc}^{FeCO_3})^2 + c(X_{Cc}^{FeCO_3}/X_{Cc}^{MgCO_3}) + d(X_{Cc}^{FeCO_3}\cdot X_{Cc}^{MgCO_3}) + e(X_{Cc}^{FeCO_3}/X_{Cc}^{MgCO_3})^2 + f(X_{Cc}^{FeCO_3}\cdot X_{Cc}^{MgCO_3})^2 \quad (T, \mathrm{K}), \qquad (31)$$

where T^{Mg} is the temperature for the pure $CaCO_3$-$MgCO_3$ system calculated from equation (23) using $MgCO_3$ in the ternary calcite, and the lettered coefficients are those listed in Table 3. These coefficients have been fit from the 400, 550, and 700 °C ternary diagrams with $X_{Cc}^{FeCO_3} \leqslant 0{\cdot}08$ at 400 °C and $\leqslant 0{\cdot}20$ at 550 and 700 °C for the calcite–dolomite solvus only. Within the limits of accuracy discussed above, this empirical approach is presently preferable to the use of a K_D thermometer for calcite–ankerite pairs.

TABLE 4

Temperatures calculated for ferroan calcites in equilibrium with dolomite/ankerite from equation (31, this study) and the correction of Bickle & Powell (1977). The Bickle & Powell temperatures have been referenced to our calibration of the iron-free solvus (equation 20).

	*Composition**			*Temperature (K)*			
Source	$CaCO_3$	$MgCO_3$	$FeCO_3$	*1*	*2*	*3*	*4*
Klein (1978)	0·784	0·052	0·164	950	(1010)	—	910
Klein (1978)	0·762	0·051	0·187	950	(1040)	—	910
Klein (1978)	0·836	0·066	0·098	950	(970)	—	930
Pinsent & Smith (1975)	0·965	0·015	0·020	650	640	620	620
Sobol (1973)	0·929	0·042	0·029	850	820	770	800

* All compositions normalized to $CaCO_3 + MgCO_3 + FeCO_3 = 1{\cdot}0$.

(1) Estimated from metamorphic grade. Temperatures given are ± 50 °C, (2) Bickle & Powell (1977), (3) Powell *et al.* (1984), (4) This Study. Dashed values for the Powell *et al.* thermometer are for compositions outside the range of their diagram, bracketed values under Bickle & Powell are for compositions outside of their recommended range of iron contents.

A series of temperatures calculated from our model and those of Bickle & Powell (1977) and Powell *et al.* (1984) are compared for several published analyses of iron-bearing calcites in equilibrium with dolomite (Table 4). In order to facilitate the direct comparison of the iron correction, Bickle & Powell's temperatures have been referenced to our calibration of the iron-free calcite–dolomite solvus (equation 23). Bickle & Powell's correction is systematically higher than ours by approximately 7 °C per mol per cent $X_{Cc}^{FeCO_3}$. Given the large numbers of assumptions necessary to both calibrations a disagreement of this magnitude is not unexpected. The results from the Powell *et al.* thermometer were taken directly from their fig. 3, and only compositions which fall within this figure were considered. Based on the limited

results shown, the Powell *et al.* thermometer appears to give lower temperatures than ours, especially for higher iron and magnesium contents. A careful experimental calibration of this ternary solvus is necessary for a more accurate calibration.

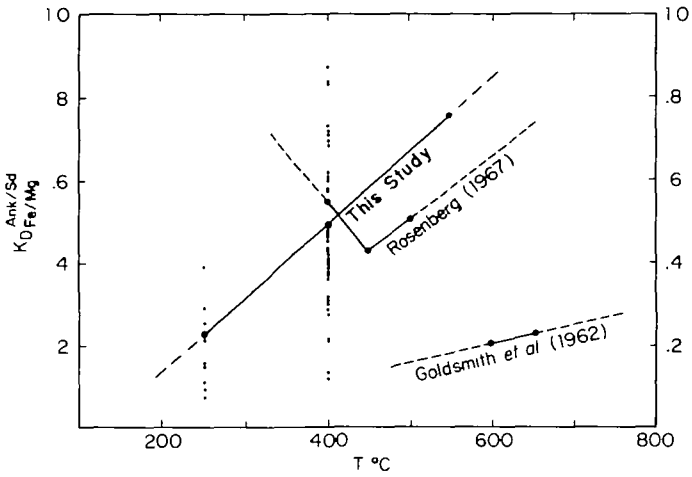

FIG. 15. Values of K_D $(X^{FeCO_3}/X^{MgCO_3})_{Ank}/(X^{FeCO_3}/X^{MgCO_3})_{Sd}$ vs. temperature calculated from natural assemblages. K_D values calculated from Goldsmith *et al.* (1962), Rosenberg (1967), and this study along the edge of the three-phase field are shown.

Siderite–Ankerite Thermometry

The siderite–ankerite solvus has received far less attention than the calcite–ankerite solvus as a potential geothermometer. The calibration of Talantsev & Sazonov (1979), which assumed that the differences between Rosenberg's and Goldsmith *et al.*'s results are due to pressure, is of questionable validity. The mole fraction of $MgCO_3$ in both siderite and dolomite on this solvus appear to change slowly with temperature (Figs. 6–10), and thus may be inappropriate for thermometry. Calculations of K_D derived from the analyses of natural carbonates (Fig. 15) suggest an increase in K_D with temperature. Rosenberg's (1967) results agree more closely with this trend than do those of Goldsmith *et al.* (1962), but Rosenberg's results suggest a change in slope of K_D vs. T at 400 °C. While such a change is not impossible, such complexity is not supported by the data. In fitting our ternary model we forced the K_D vs. T function:

$$K_D = \frac{(X^{FeCO_3}/X^{MgCO_3})_{Ank}}{(X^{FeCO_3}/X^{MgCO_3})_{Sd}} = -0{\cdot}691 + 0{\cdot}00176\ T\ (T, \text{K}) \qquad (32)$$

to be linear and to fit the average values at each temperature. The large scatter in the natural data, however, suggests that this will not be an accurate thermometer. The scatter may be partially due to the low Ca-content of the natural siderites relative to the calculated edge of the two-phase region. As the calculation is strongly constrained by the positions of the calcite-siderite and dolomite–magnesite solvi, compositions of the natural siderites may have reset. Thus, carefully reversed experimental data are necessary to calibrate K_D thermometers for coexisting carbonates, and natural pairs must be evaluated in terms of resetting.

ACKNOWLEDGEMENTS

The authors thank Dr. D. R. Peacor for a critical reading of this manuscript, and Dr. C. Klein for helpful conversations about iron-carbonates. J. R. Goldsmith, R. Powell, R. Reeder, J. M. Rice, R. Sack, S. K. Saxena, and B. J. Wood, provided helpful critical reviews. Dr. Sack's comments on the ankerite/siderite K_D problem were especially helpful. NSF grant EAR-8009538 to E.J.E. is acknowledged for support of some of this work. The Geological Society of America, Sigma Xi, and the Scott Turner Fund provided research support, and the University of Michigan provided microprobe and computing facilities. We also thank Mr. Ed Berdusco and the Algoma Ore Co. at Wawa, Ontario for providing access to their properties. Ms. Mary Schatz is gratefully thanked for her patience during repeated retypings of the manuscript.

REFERENCES

Ackermand, D., & Morteani, G., 1972. Mikrosondenuntersuchungen an Ankeritisch Entmischten Calciten aus den Mittleren Zillertaler Alpen. *Contr. Miner. Petrol.* **36,** 147–54.

Barron, B. J., 1974. The use of coexisting calcite-ankerite solid solutions as a geothermometer. *Ibid.* **47,** 77–80.

Beran, A., & Zemann, J., 1977. Refinement and comparison of the crystal structure of a dolomite and an iron-rich ankerite. *Tschermaks Min. Petrogr. Mitt.* **24,** 279–86.

Bickle, M. J., & Powell, R., 1977. Calcite-dolomite geothermometry for iron-bearing carbonates: The Glockner area of the Tauern window, Austria. *Contr. Miner. Petrol.* **59,** 281–92.

Bischoff, W. D., Bishop, F. C., & Mackenzie, F. T., 1983. Biogenically produced magnesian calcite: Inhomogeneities in chemical and physical properties of biogenic magnesian calcite: comparison with synthetic phases. *Am. Miner.* **68,** 1183–8.

Böhlke, J. K., 1986. Local wall rock control of alteration and mineralization reactions along discordant gold quartz veins, Alleghany, California. *Ph.D. thesis, University of California, Berkeley.*

Bowman, J. R., 1978. Contact metamorphism, skarn formation and origin of the C–O–H skarn fluids in the Black Butte Aureole, Elkhorn, Montana, *Ph.D. thesis, University of Michigan.*

——& Essene, E. J., 1982. *P–T–X*(CO_2) conditions of contact metamorphism in the Black Butte aureole, Elkhorn, Montana. *Am. J. Sci.* **282,** 311–40.

Burton, B., & Kikuchi, R., 1984. Thermodynamic analysis of the system $CaCO_3$-$MgCO_3$ in the tetrahedron approximation of the Cluster Variation Method. *Am. Miner.* **69,** 165–75.

Butler, P., 1969. Mineral compositions and equilibria in the metamorphosed iron-formation of the Gagnon region, Quebec, Canada. *J. Petrology,* **10,** 56–101.

Byrnes, A. P., & Wyllie, P. J., 1981. Subsolidus and melting relations for the join $CaCO_3$-$MgCO_3$ at 10 kb. *Geochim. cosmochim. Acta,* **45,** 321–8.

Carpenter, M. A., & Putnis, A., 1985. Cation order and disorder during crystal growth: Some implications for natural mineral assemblages. In: Thompson, A. B. and Rubie, D. C. (eds.). *Metamorphic Reactions: Kinetics, Textures and Deformation. Advances in Physical Geochemistry* **4,** 1–26.

Davidson, P. M., 1984. Thermodynamic analysis of quadrilateral pyroxenes and olivines. *Ph.D. thesis, SUNY, Stony Brook.*

Dietrich, H., 1983. Zur Petrologie und Metamorphose des Brennermesozoikums (Stubaier Alpen, Tirol). *Tschermaks Min. Petrogr. Mitt.* **31,** 235–58.

Essene, E. J., 1983. Solid solutions and solvi among metamorphic carbonates with applications to geologic thermometry. In: Reeder, R. J. (ed.). *Carbonates: Mineralogy and Chemistry. MSA Reviews in Mineralogy,* **11,** 77–96.

Floran, R. J., & Papike, J. J., 1975. Petrology of the low-grade rocks of the Gunflint Iron-Formation, Ontario-Minnesota. *Bull. geol. Soc. Am.* **86,** 1169–90.

Frost, M. T., 1982. The magnesite deposit at Main Creek, Savage River, Tasmania. *Econ. Geol.* **77,** 1901–11.

Fyfe, W. S., & Verhoogen, J., 1958. General thermodynamic considerations. In: Fyfe, W. S., Turner, F. J., & Verhoogen, J. (ed.). *Metamorphic Reactions and Metamorphic Facies. Geol. Soc. Amer. Memoir* **73.**

Ganguly, J., & Saxena, S. K., 1984. Mixing properties of aluminosilicate garnets: constraints from natural and experimental data and applications to geothermo-barometry. *Am. Miner.* **69,** 88–97.

Goldsmith, J. R., 1983. Phase relations or rhombohedral carbonates. In: Reeder, R. J. (ed.). *Carbonates: Mineralogy and Chemistry. MSA Reviews in Mineralogy* **11,** 49–76.

——& Graf, D. L., 1958. Structural and compositional variations in some natural dolomites. *J. Geol.* **66,** 678–93.

——————Witters, J., & Northrup, D. A., 1962. Studies in the system $CaCO_3$-$MgCO_3$-$FeCO_3$: A method for major-element spectrochemical analysis; 3. Composition of some ferroan dolomites. *J. Geol.* **70,** 659–87.

——Heard, H. C., 1961. Subsolidus phase relations in the system $CaCO_3$-$MgCO_3$. *Ibid.* **69,** 45–74.

——Newton, R. C., 1969. *P–T–X* relations in the system $CaCO_3$-$MgCO_3$ at high temperatures and pressures. *Am. J. Sci.* **267A,** 160–90.

Gordon, T. M., & Greenwood, H. J., 1970. The reaction: dolomite + quartz + water = talc + calcite + carbon dioxide. *Am. J. Sci.* **26B**, 225-42.

Graf, D. L., & Goldsmith, J. C., 1955. Dolomite-magnesian calcite relations at elevated temperatures and CO_2 pressures. *Am. Miner.* **51**, 353-80.

——— 1958. The solid solubility of $MgCO_3$ in $CaCO_3$: A revision. *Geochim. Cosmochim. Acta*, **13**, 218-19.

Grummon, M. L., 1977. Experimental techniques for studying reaction equilibria at elevated temperatures and pressures. *M.S. thesis, University of Michigan.*

Haase, C. S., 1979. Metamorphic petrology of the Negaunee Iron Formation, Marquette District, Northern Michigan. *Ph.D. thesis, Indiana University.*

Hall, R. D., 1980. Metamorphism of sulfide schists, Limerick township, Ontario. *Ph.D. thesis, University of Western Ontario.*

Harker, R. I., & Tuttle, O. F., 1955. Studies in the system $CaO-MgO-CO_2$, Part 2: Limits of solid solution along the binary join $CaCO_3-MgCO_3$. *Am. J. Sci.* **253**, 274-82.

Hatcher, R. D., Price, V. Jr., & Snipes, P. S., 1973. Analysis of chemical and paleotemperature data from selected rocks of the Southern Appalachians. *Southeastern Geol.* **15**, 55-70.

Holland, T. J. B., Navrotsky, A., & Newton, R. C., 1980. Thermodynamic parameters of $CaMgSi_2O_6-Mg_2Si_2O_6$ pyroxenes based on regular solution and cooperative disordering models by Holland, Navrotsky, and Newton (1979): Reply to Lindsley and Davidson (1980). *Contr. Miner. Petrol.* **75**, 305-6.

Hutcheon, I., & Moore, J. M., 1973. The tremolite isograd near Marble Lake, Ontario. *Can. J. Earth Sci.* **10**, 936-47.

Irving, A. J., & Wyllie, P. J., 1975. Subsolidus and melting relationships for calcite, magnesite, and the join $CaCO_3-MgCO_3$ to 36 kb. *Geochim. cosmochim. Acta*, **39**, 35-53.

Klein, C., 1966. Mineralogy and petrology of the metamorphosed Wabush Iron Formation, southwestern Labrador. *J. Petrology*, **7**, 246-305.

—— 1974. Greenalite, stilpnomelane, minnesotaite, crocidolite, and carbonates in a very low-grade metamorphic Precambrian iron-formation. *Can. Miner.* **12**, 475-98.

—— 1978. Regional metamorphism of Proterozoic iron-formation, Labrador Trough, Canada. *Am. Miner.* **63**, 898-912.

—— & Fink, R. P., 1976. Petrology of the Sokoman Iron Formation in the Howells River area, at the western edge of the Labrador Trough. *Econ. Geol.* **71**, 453-87.

—— & Gole, M., 1981. Mineralogy and petrology of parts of the Marra Mamba Iron-Formation, Hammersley Basin, Western Australia. *Am. Miner.* **66**, 507-25.

Kretz, R., 1980. Occurrence, mineral chemistry, and metamorphism of Precambrian rocks in a portion of the Grenville province. *J. Petrology*, **21**, 573-620.

Lesher, C. M., 1978. Mineralogy and petrology of the Sokoman Iron Formation near Ardua Lake, Quebec. *Can. J. Earth Sci.* **15**, 480-500.

Lindsley, D. H., Grover, J. E., & Davidson, P. M., 1981. The thermodynamics of the $Mg_2Si_2O_6-CaMgSi_2O_6$ join. A review and an improved model. In: Newton, R. C., Navrotsky, A., & Wood, B. J. (eds.). *Thermodynamics of Minerals and Melts, Advances in Physical Chemistry*, 1 Springer-Verlag.

Machamer, J. F., 1968. Geology and origin of the iron ore deposits of the Zenith mine, Vermillion district, Minnesota. *Minn. Geol. Surv. Spec. Publ. Ser. SP-2*, 1-56.

Miyano, T., 1978. Phase relations in the system Fe-Mg-Si-O-H and environments during low-grade metamorphism of some Precambrian iron-formations. *J. geol. Soc. Jap.* **84**, 679-90.

Navrotsky, A., & Loucks, D., 1977. Calculation of subsolidus phase relations in carbonates and pyroxenes. *Phys chem. Miner.* **1**, 109-27.

Nesbitt, B. E., 1979. Regional metamorphism of the Ducktown, Tennessee massive sulfide and adjoining portions of the Blue Ridge Province. *Ph.D. thesis, University of Michigan.*

—— Essene, E. J., 1982. Metamorphic thermometry and barometry of a portion of the southern Blue Ridge province. *Am. J. Sci.*, **282**, 701-29.

Pakkala, Y., & Puustinen, K., 1978. The chromian marbles of the Kittila, Finnish Lapland. *Bull. geol. Soc. Fin.* **50**, 15-29.

Pearson, M. J., 1974. Sideritic concretions from the Westphalian of Yorkshire: A chemical investigation of the carbonate phase. *Miner. Mag.* **39**, 696-9.

Perkins, D. III, Essene, E. J., & Marcotty, L. A., 1982. Thermometry and barometry of some amphibolite-granulite facies rocks from the Otter Lake area, southern Quebec. *Can. J. Earth Sci.* **19**, 1759-74.

Pinsent, R. H., & Smith, D. G. W., 1975. The development of carbonate bearing biotite isograd assemblages from Tete Jaune Cache, British Colombia, Canada. *Can. Miner.* **13**, 151-61.

Powell, R., Condliffe, D. M., & Condliffe, E., 1984. Calcite-dolomite geothermometry in the system $CaCO_3-MgCO_3-FeCO_3$: An experimental study. *J. metamorphic Geol.* **2**, 33-42.

Puhan, D., 1976. Metamorphic temperature determined by means of the dolomite-calcite solvus geothermometer: Examples from the central Damara orogen (Southwest Africa). *Contr. Miner. Petrol.* **59**, 237-59.

Reeder, R. J., 1983. Crystal chemistry of the rhombohedral carbonates. In: Reeder, R. J. (ed.). *Carbonates: Mineralogy and Chemistry. MSA Reviews in Mineralogy*, **11**, 1-47.

—— Nakajima, Y., 1982. The nature of ordering and ordering defects in dolomite. *Phys. chem. Miner.* **8**, 29-35.

——— & Wenk, H. R., 1983. Exsolution structure in calcian dolomites. *Am. Miner.* **68**, 769-76.

Rice, J. M., 1977. Contact metamorphism of impure dolomitic limestone in the Boulder aureole, Montana. *Contr. Miner. Petrol.* **59**, 237–59.

Robie, R. A., Haselton, H. T., & Hemingway, B. S., 1984. Low temperature heat capacities and entropies of rhodochrosite ($MnCO_3$) and siderite ($FeCO_3$) between 5 and 600 K. *Am. Miner.* **69**, 349–57.

—— Hemingway, B. S., & Fisher, J. R., 1978. Thermodynamic properties of minerals and related substances at 298·15 K and 1 bar (10^5 Pa) pressure and at higher temperatures. *Bull. U.S. geol. Surv.* 1452.

Rosenberg, P. E., 1960. Subsolidus studies in the system $CaCO_3$-$MgCO_3$-$FeCO_3$-$MnCO_3$. *Ph.D. thesis, Pennsylvania State University.*

——1963*a*. Subsolidus relations in the system $CaCO_3$-$FeCO_2$. *Am. J. Sci.* **261**, 683–90.

——1963*b*. Synthetic solid solutions in the systems $MgCO_3$-$FeCO_3$ and $MnCO_3$-$FeCO_3$. *Am. Miner.*, **48**, 1396–400.

——1967. Subsolidus relations in the system $CaCO_3$-$MgCO_3$-$FeCO_3$ between 350 and 550 °C. *Ibid.* **52**, 787–97.

Sanford, R. F., 1982. Growth of ultramafic reaction zones in greenschist to amphibolite facies metamorphism. *Am. J. Sci.* **282**, 543–616.

Saxena, S. K., 1973. Thermodynamics of rock-forming crystalline solutions. *Minerals, Rocks, and Inorganic Materials: Monograph Series of Theoretical and Experimental Studies, Vol. 8*, von Engelhardt, W., Hahn, T., Roy, R., & Wyllie, P. J. (eds.). New York: Springer-Verlag.

Schultz-Güttler, R., 1986. The influence of disordered, non-equilibrium dolomites and the Mg-solubility in calcite in the system $CaCO_3$-$MgCO_3$. *Contr. Miner. Petrol.* **93**, 395–8.

Shibuya, G., & Harada, S., 1976. Mineralogical studies on kutnahorite and other carbonate minerals from the Hoei Mine, Oita prefecture. *J. miner. Soc. Jap.* **13**, 1–25.

Skippen, G., 1974. An experimental model for low pressure metamorphism of siliceous dolomitic marble. *Am. J. Sci.* **274**, 487–509.

Sobol, J. W., 1973. The petrology of Grenville marbles in the vicinity of Bancroft, Ontario. *M.S. thesis, University of Michigan.*

Suzuki, K., 1977. Local equilibrium during the contact metamorphism of siliceous dolomites in Kasuga-Mura, Gifu-ken, Japan. *Contr. Miner. Petrol.* **61**, 79–89.

Talantsev, A. S., 1976. Dolomite-calcite geothermobarometer. *Dokl. Earth Sci. Sect.* **228**, 166–8.

——1978. Revision of the calcite-dolomite geothermobarometer. *Geochem. Int.* **15**, 108–16.

—— & Sazonov, V. N., 1979. Variatzzii sostavov sosushchesttvuyuschich dolomit–ankerita i magnezit–siderita kak pokazatel *P–T*-uislovii mineraloobrazovaniya. (Variations in compositions of coexisting dolomite–ankerite and magnesite–siderite as an index of PT-conditions of mineral formation.) *Akad. Nauk SSSR Ural'skii Nauchaii Tzentr*, 95–103. [In Russian.]

Treiman, A. H., & Essene, E. J., 1983. A periclase–dolomite–calcite carbonatite from the Oka Complex, and its calculated volatile composition. *Contr. Miner. Petrol.* **85**, 149–57.

Valley, J. W., 1980. The role of fluids during metamorphism of marbles and associated rocks in the Adirondack Mountains, New York. *Ph.D. thesis, University of Michigan.*

Wada, H., & Suzuki, K., 1983. Carbon isotopic thermometry calibrated by dolomite–calcite solvus temperatures. *Geochim. cosmochim. Acta*, **47**, 697–706.

Wohl, K., 1953. Thermodynamic evaluation of binary and ternary liquid systems. *Chem. Eng. Prog.* **49**, 218–19.

APPENDIX

$$
\begin{aligned}
\Delta\mu^{CaCO_3}_{Dol\text{-}Cc} = RT\ln\left[\frac{X^{CaCO_3}_{Cc}}{X^{CaCO_3}_{Dol}}\right]
&+ ((X^{MgCO_3}_{Cc})^2\,(W^{CaMg}_{Cc} + 2X^{CaCO_3}_{Cc}(W^{MgCa}_{Cc} - W^{CaMg}_{Cc}))\\
&+ (X^{FeCO_3}_{Cc})^2\,(W^{CaFe}_{Cc} + 2X^{CaCO_3}_{Cc}(W^{FeCa}_{Cc} - W^{CaFe}_{Cc}))\\
&+ (X^{MgCO_3}_{Cc}\,X^{FeCO_3}_{Cc})\,[(W^{MgCa}_{Cc} + W^{CaMg}_{Cc} + W^{FeCa}_{Cc} + W^{CaFe}_{Cc} - W^{MgFe}_{Cc} - W^{FeMg}_{Cc})/2\\
&+ X^{CaCO_3}_{Cc}(W^{MgCa}_{Cc} - W^{CaMg}_{Cc} + W^{FeCa}_{Cc} - W^{CaFe}_{Cc}) + (X^{MgCO_3}_{Cc} - X^{FeCO_3}_{Cc})(W^{MgFe}_{Cc} - W^{FeMg}_{Cc})\\
&- (1 - 2X^{CaCO_3}_{Cc})\,C_{Cc}]\\
&- ((X^{MgCO_3}_{Dol})^2\,(W^{CaMg}_{Dol} + 2X^{CaCO_3}_{Dol}(W^{MgCa}_{Dol} - W^{CaMg}_{Dol}))\\
&+ (X^{FeCO_3}_{Dol})^2\,(W^{CaFe}_{Dol} + 2X^{CaCO_3}_{Dol}(W^{FeCa}_{Dol} - W^{CaFe}_{Dol}))\\
&+ (X^{MgCO_3}_{Dol}\,X^{FeCO_3}_{Dol})\,[(W^{MgCa}_{Dol} + W^{CaMg}_{Dol} + W^{FeCa}_{Dol} + W^{CaFe}_{Dol} - W^{MgFe}_{Dol} - W^{FeMg}_{Dol})/2\\
&+ X^{CaCO_3}_{Dol}(W^{MgCa}_{Dol} - W^{CaMg}_{Dol} + W^{FeCa}_{Dol} - W^{CaFe}_{Dol}) + (X^{MgCO_3}_{Dol} - X^{FeCO_3}_{Dol})(W^{MgFe}_{Dol} - W^{FeMg}_{Dol})\\
&- (1 - 2X^{CaCO_3}_{Dol})\,C_{Dol}]\,. \qquad (19)
\end{aligned}
$$

$$\Delta\mu^{MgCO_3}_{Dol\text{-}Cc} = RT\ln\left[\frac{X^{MgCO_3}_{Cc}}{X^{MgCO_3}_{Dol}}\right] + ((X^{FeCO_3}_{Cc})^2 (W^{MgFe}_{Cc} + 2X^{MgCO_3}_{Cc} (W^{FeMg}_{Cc} - W^{MgFe}_{Cc}))$$
$$+ (X^{CaCO_3}_{Cc})^2 (W^{MgCa}_{Cc} + 2X^{MgCO_3}_{Cc}(W^{CaMg}_{Cc} - W^{MgCa}_{Cc}))$$
$$+ (X^{FeCO_3}_{Cc} X^{CaCO_3}_{Cc}) [(W^{FeMg}_{Cc} + W^{MgFe}_{Cc} + W^{CaMg}_{Cc} + W^{MgCa}_{Cc} - W^{FeCa}_{Cc} - W^{CaFe}_{Cc}) / 2$$
$$+ X^{MgCO_3}_{Cc} (W^{FeMg}_{Cc} - W^{MgFe}_{Cc} + W^{CaMg}_{Cc} - W^{MgCa}_{Cc}) + (X^{FeCO_3}_{Cc} - X^{CaCO_3}_{Cc}) (W^{FeCa}_{Cc} - W^{CaFe}_{Cc})$$
$$- (1 - 2X^{MgCO_3}_{Cc}) C_{Cc}]$$
$$- ((X^{FeCO_3}_{Dol})^2 (W^{MgFe}_{Dol} + 2X^{MgCO_3}_{Dol}(W^{FeMg}_{Dol} - W^{MgFe}_{Dol}))$$
$$+ (X^{CaCO_3}_{Dol})^2 (W^{MgCa}_{Dol} + 2X^{MgCO_3}_{Dol}(W^{CaMg}_{Dol} - W^{MgCa}_{Dol}))$$
$$+ (X^{FeCO_3}_{Dol} X^{CaCO_3}_{Dol}) [(W^{FeMg}_{Dol} + W^{MgFe}_{Dol} + W^{CaMg}_{Dol} + W^{MgCa}_{Dol} - W^{FeCa}_{Dol} - W^{CaFe}_{Dol}) / 2$$
$$+ X^{MgCO_3}_{Dol} (W^{FeMg}_{Dol} - W^{MgFe}_{Dol} + W^{CaMg}_{Dol} - W^{MgCa}_{Dol}) + (X^{FeCO_3}_{Dol} - X^{CaCO_3}_{Dol}) (W^{FeCa}_{Dol} - W^{CaFe}_{Dol})$$
$$- (1 - 2X^{MgCO_3}_{Dol}) C_{Dol}]. \quad (20)$$

$$\Delta\mu^{FeCO_3}_{Dol\text{-}Cc} = RT\ln\left[\frac{X^{FeCO_3}_{Cc}}{X^{FeCO_3}_{Dol}}\right] + ((X^{CaCO_3}_{Cc})^2 (W^{FeCa}_{Cc} + 2X^{FeCO_3}_{Cc} (W^{CaFe}_{Cc} - W^{FeCa}_{Cc}))$$
$$+ (X^{MgCO_3}_{Cc})^2 (W^{FeMg}_{Cc} + 2X^{FeCO_3}_{Cc}(W^{MgFe}_{Cc} - W^{FeMg}_{Cc}))$$
$$+ (X^{CaCO_3}_{Cc} X^{MgCO_3}_{Cc}) [(W^{CaFe}_{Cc} + W^{FeCa}_{Cc} + W^{MgFe}_{Cc} + W^{FeMg}_{Cc} - W^{CaMg}_{Cc} - W^{MgCa}_{Cc}) / 2$$
$$+ X^{FeCO_3}_{Cc} (W^{CaFe}_{Cc} - W^{FeCa}_{Cc} + W^{MgFe}_{Cc} - W^{FeMg}_{Cc}) + (X^{CaCO_3}_{Cc} - X^{MgCO_3}_{Cc}) (W^{CaMg}_{Cc} - W^{MgCa}_{Cc})$$
$$- (1 - 2X^{FeCO_3}_{Cc}) C_{Cc}]$$
$$- ((X^{CaCO_3}_{Dol})^2 (W^{FeCa}_{Dol} + 2X^{FeCO_3}_{Dol}(W^{CaFe}_{Dol} - W^{FeCa}_{Dol}))$$
$$+ (X^{MgCO_3}_{Dol})^2 (W^{FeMg}_{Dol} + 2X^{FeCO_3}_{Dol}(W^{MgFe}_{Dol} - W^{FeMg}_{Dol}))$$
$$+ (X^{CaCO_3}_{Dol} X^{MgCO_3}_{Dol}) [(W^{CaFe}_{Dol} + W^{FeCa}_{Dol} + W^{MgFe}_{Dol} + W^{FeMg}_{Dol} - W^{CaMg}_{Dol} - W^{MgCa}_{Dol}) / 2$$
$$+ X^{FeCO_3}_{Dol} (W^{CaFe}_{Dol} - W^{FeCa}_{Dol} + W^{MgFe}_{Dol} - W^{FeMg}_{Dol}) + (X^{CaCO_3}_{Dol} - X^{MgCO_3}_{Dol}) (W^{CaMg}_{Dol} - W^{MgCa}_{Dol})$$
$$- (1 - 2X^{FeCO_3}_{Dol}) C_{Dol}]. \quad (21)$$

1989 IAVCEI ASSEMBLY

The 1989 IAVCEI Assembly will be held in Santa Fe, New Mexico (25 June–1 July). The scientific program, organized around the general theme of *Continental Magmatism* will emphasize volcanology and geochemistry–petrology. Main symposium topics are: Continental Arc Volcanism, Intraplate Alkalic Volcanism, Continental Rift and Flood Basalt Volcanism, Geothermal Energy and Metallogenesis, Active Volcanism and Volcanic Hazards, Explosive Volcanism and Physical Volcanology, Petrologic Evolution of Continental Magmas, and Planetary Volcanism. An extensive menu of 18 field excursions throughout the western USA will be offered.

Individuals interested in attending this meeting, who have not received a copy of the First Circular, should write to:

IAVCEI/1989
Protocol Office, Mail Code P-366
Los Alamos National Laboratory
Los Alamos, N.M. 87545

Please request addition of your name (plus names of colleagues and students who might attend) to the mailing list for the Second and Third Circulars, and a copy of the First Circular. The First Circular contains much more information concerning the program and field excursions plus preliminary details about accommodation, costs, publications, financial aid, additional activities, and a questionnaire which we strongly urge you to complete and return.